

1 Global soil nitrous oxide emissions in a dynamic carbon- 2 nitrogen model

3 Y. Y. Huang¹ and S. Gerber¹

4 [1] {Soil and Water Science Department, Institute of Food and Agricultural Sciences,
5 University of Florida, Gainesville, Florida 32611 }

6 Correspondence to: S. Gerber (sgerber@ufl.edu)

7

8 **Abstract**

9 Nitrous oxide (N₂O) is an important greenhouse gas that also contributes to the depletion of
10 stratospheric ozone. Due to its high temporal and spatial heterogeneity, a quantitative
11 understanding of terrestrial N₂O emission, its variabilities and responses to climate change is
12 challenging. We added a soil N₂O emission module to the dynamic global land model LM3V-
13 N, and tested its sensitivity to mechanisms that affect the level of mineral N in soil such as plant
14 N uptake, biological N fixation, amount of volatilized N redeposited after fire, and nitrification.
15 We further tested the relationship between N₂O emission and soil moisture, and finally assessed
16 responses to elevated CO₂ and temperature. Results extracted from the corresponding gridcell
17 (without site-specific forcing data) were comparable with the average of cross-site observed
18 annual mean emissions, although differences remained across individual sites if stand-level
19 measurements were representative of gridcell emissions. Processes, such as plant N uptake and
20 N loss through fire volatilization, that regulate N availability for nitrification-denitrification
21 have strong controls on N₂O fluxes in addition to the parameterization of N₂O loss through
22 nitrification and denitrification. Modelled N₂O fluxes were highly sensitive to water filled pore
23 space (WFPS), with a global sensitivity of approximately 0.25 TgN per year per 0.01 change
24 in WFPS. We found that the global response of N₂O emission to CO₂ fertilization was largely
25 determined by the response of tropical emissions with reduced N₂O fluxes in the first few
26 decades and increases afterwards. The initial reduction was linked to N limitation under higher
27 CO₂ level, and was alleviated through feedbacks such as biological N fixation. The extratropical
28 response was weaker and generally positive, highlighting the need to expand field studies in
29 tropical ecosystems. Warming generally enhanced N₂O efflux, and the enhancement was
30 greatly dampened when combined with elevated CO₂, although CO₂ alone had a small effect.

1 Our analysis suggests caution when extrapolation from current field CO₂ enrichment and
2 warming studies to the global scale.

3

4 **1 Introduction**

5 Nitrous oxide (N₂O) is a major reactant in depleting stratospheric ozone as well as an important
6 greenhouse gas (Ravishankara et al., 2009; Butterbach-Bahl et al., 2013; Ciais et al., 2013). With
7 a global warming potential of 298 times more (per unit mass) than that of carbon dioxide (CO₂)
8 over a 100-year period (Forster et al., 2007), the contributions of N₂O emissions to global
9 radiative forcing and climate change are of critical concern (Zaehle and Dalmonech, 2011). The
10 concentration of atmospheric N₂O has been increasing considerably since the industrial
11 revolution with a linear rate of 0.73 ± 0.03 ppb yr⁻¹ over the last three decades (Ciais et al., 2013).
12 Although applications of synthetic fertilizer and manure during agriculture intensification have
13 been identified as the major causes of this increase which has resulted in an increase of the
14 radiative forcing by 0.125 W m^{-2} (Davidson, 2009; Zaehle and Dalmonech, 2011; Zaehle et al.,
15 2011), nonagricultural (natural) soil is still an important N₂O source (Ciais et al., 2013; Syakila
16 and Kroeze, 2011). N₂O fluxes from nonagricultural soils are highly heterogeneous, which
17 limits our ability to estimate and predict global scale budget, and quantify its response to global
18 environmental changes (Butterbach-Bahl et al., 2013; Ciais et al., 2013).

19 Most of the N₂O fluxes from soil are produced by microbial nitrification and denitrification
20 (Braker and Conrad, 2011; Syakila and Kroeze, 2011). Nitrification is an aerobic process that
21 oxidizes ammonium (NH₄⁺) to nitrate (NO₃⁻), during which some N is lost as N₂O.
22 Denitrification reduces nitrate or nitrite to gaseous N (i.e. NO_x, N₂O and N₂), a process that is
23 fostered under anaerobic conditions. N₂O is generated in intermediary steps during
24 denitrification and a small portion can escape from soil before further reduction to N₂ takes
25 place. Soil texture, soil NH₄⁺, soil water filled pore space (WFPS), mineralization rate, soil pH,
26 and soil temperature are well-known regulators of nitrification N₂O fluxes (Parton et al.,
27 1996; Li et al., 2000; Parton et al., 2001). Denitrification and associated N₂O emissions depend
28 primarily on carbon supply, the redox potential and soil NO₃⁻ (Firestone and Davidson,
29 1989; Parton et al., 1996). Soil moisture has a particularly strong impact (Galloway et al.,
30 2003; Schlesinger, 2009) as it influences nitrification and denitrification rates through its
31 regulations on substrate availability and soil redox potential (as oxygen diffusion proceeds at
32 much slower rate in water filled than in air filled pore space), thereby also controlling the

1 partitioning among various denitrification products (i.e. NO_x , N_2O and N_2) (Firestone and
2 Davidson, 1989;Parton et al., 2001). Although emissions are known to be sensitive to soil
3 moisture, quantitative understanding of its role in terrestrial N_2O fluxes and variability is limited
4 (Ciais et al., 2013).

5 At regional to global scale, the application of the “hole-in-pipe” concept (Firestone and
6 Davidson, 1989) in the CASA biosphere model pioneered one of the earliest process-based
7 estimation of natural soil N_2O fluxes. The model calculated the sum of NO , N_2O and N_2 fluxes
8 as a constant portion of gross mineralized N, and the relative ratios of N trace gases
9 ($\text{NO}_x:\text{N}_2\text{O}:\text{N}_2$) as a function of soil moisture (Potter et al., 1996). While the early models of
10 nitrification and denitrification are primarily conceptual driven, recent global N_2O models
11 combine advancements in global dynamic land models with more detailed processes, including
12 microbial dynamics. Xu-Ri and Prentice (2008) simplified nitrification and denitrification
13 modules from DNDC (i.e., DeNitrification-DeComposition) (Li et al., 1992;Li et al., 2000) in
14 their global scale dynamic N scheme (DyN) and incorporated DyN into the LPJ dynamic global
15 vegetation model. In the DNDC approach, nitrification and denitrification were allowed to
16 happen simultaneously in aerobic and anaerobic microsites. Zaehle et al. (2011) incorporated a
17 nitrification-denitrification scheme into the O-CN land model following largely the LPJ-DyN
18 with minor modifications and additions of the effects of soil pH and chemo-denitrification that
19 originated from DNDC (Li et al., 2000). Stocker et al. (2013) embeded the LPJ-DyN approach
20 into an Earth System Model and investigated the feedbacks of N_2O emissions, together with
21 CO_2 and CH_4 , to climate. Compared to LPJ-DyN approach, Saikawa et al. (2013) retained the
22 explicit simulation of nitrifying and denitrifying bacteria from DNDC in their CLMCN- N_2O
23 module based on CLM V3.5 land model. Simulations with O-CN demonstrated a positive
24 response of N_2O emissions to historical warming and a negative response to historical CO_2
25 increase, globally. While CO_2 and interaction with climate change resulted in an increase in
26 historical and future N_2O emissions from LPJ-DyN (Xu-Ri et al., 2012) and its application in
27 LPX-Bern (Stocker et al., 2013), respectively, historical CO_2 change alone, i.e. single factor of
28 Xu-Ri et al., (2012), caused a slight decrease in historical N_2O emissions. The negative CO_2
29 response seems to be in disagreement with one meta-analysis of manipulative field experiments
30 showing an increase in N_2O emissions at elevated levels of CO_2 (Zaehle et al., 2011;Xu-Ri et
31 al., 2012;van Groenigen et al., 2011). The discrepancy in response to global change factors
32 needs to be addressed both in models and in the interpretation of manipulative field experiments.

33

1 Here we add a N₂O gas emission module to LM3V-N, a land model developed at the Geophysical
2 Fluid Dynamics Laboratory (GFDL). In this paper, we will first briefly introduce LM3V-N and
3 describe the added N₂O emission module. We then subject the model to historic changes in CO₂,
4 N deposition, and recent climate change to infer natural N₂O emissions in the past few decades.
5 We test the model's sensitivity to soil water regime, by addressing the parameterization of soil
6 WFPS, and by replacing the model soil moisture with two different soil moisture reanalysis
7 products. We also conduct sensitivity tests with regard to the general N cycling and
8 parameterization of N₂O emissions. Since we build largely on existing parameterization of
9 nitrification-denitrification processes, our focus relies on the evaluation of these processes if
10 transferred to a different model. Finally, we subject the model to step changes in atmospheric
11 CO₂ and temperature to understand modelled responses to CO₂ fertilization/climate change.

12 **2 Methods**

13 **2.1 Model description**

14 LM3V is capable of simulating ecosystem dynamics and exchange of CO₂, water and energy
15 between land and atmosphere with the fastest time step of 30 minutes (Shevliakova et al., 2009).
16 LM3V-N expands the LM3V land model with a prognostic N cycle (Gerber et al., 2010), and
17 includes five plant functional types (PFTs): C3 and C4 grasses, tropical, temperate deciduous
18 and cold evergreen trees. Each PFT has five vegetation C pools (leaf, fine root, sapwood, labile,
19 and wood), two litter and two soil organic C pools and their corresponding N pools based on
20 the specific C:N ratios. Photosynthesis is coupled with stomatal conductance on the basis of the
21 Collatz et al., (1991,1992) simplification of the Farquhar scheme (Farquhar et al., 1980). Soil
22 hydrology in LM3V follows partly on Land Dynamics (LaD) with further improvements
23 (Shevliakova et al., 2009; Milly and Shmakin, 2002; Milly et al., 2014). N enters the ecosystem
24 through atmospheric N deposition and biological N fixation (BNF), losses via fire and leaching
25 of dissolved organic N (DON) as well as mineral N. Major characteristics of LM3V-N include
26 the following 5 aspects, and details are available in Gerber et al. (2010).

27 **2.1.1 Main characteristic of LM3V-N**

28 **2.1.1.1 C-N coupling in vegetation**

29 We briefly describe the larger plant-soil N cycle and how it links to mineral N (ammonium and
30 nitrate). Details are described in Gerber et al. (2010). Plants adjust their uptake of C and N to

1 maintain their tissue specific C:N ratios, which are PFT-dependent constants. Instead of varying
 2 C:N ratios in tissues, short-term asynchronies in C and N assimilations or temporary imbalances
 3 in stoichiometry are buffered by additional N storage pool (S) in which N is allowed to
 4 accumulate once plant N demand is satisfied. The optimum storage size S_{target} is based on tissue
 5 turnover $Q_{N,liv}$,

$$6 \quad S_{target} = t_h Q_{N,liv} \quad (1)$$

7 where t_h is the time span that buffer plant N losses (currently set as 1 year). Plant N status (x)
 8 is defined as the fraction of the actual N storage compared to the target storage: $x = S/S_{target}$.
 9 Consequently, N constraints on photosynthesis and soil N assimilation are based on plant N
 10 status:

$$11 \quad A_{g,N} = A_{g,pot}(1 - e^{-x\varphi}) \quad (2)$$

$$12 \quad U_{N,P} = U_{N,P,pot} * \begin{cases} 1 & \text{if } S < S_{target} \\ 0 & \text{else} \end{cases} \quad (3)$$

13 where $A_{g,N}$ indicates N constrained rate of gross photosynthesis ($\mu\text{molC m}^{-2} \text{s}^{-1}$) and $A_{g,pot}$
 14 corresponds to the potential photosynthetic rate without N limitation. The parameter φ mimics
 15 the metabolic deficiency as plant N decreases. $U_{N,P,pot}$ is the potential inorganic N uptake rate
 16 from soil available ammonium and nitrate pools. The actual inorganic N uptake rate ($U_{N,P}$)
 17 operates at its potential and drops to zero when N storage (S) reaches its target size.

18 **2.1.1.2 Soil C-N interactions in organic matter decomposition**

19 Organic matter decomposition is based on a modified CENTURY approach (Bolker et al.,
 20 1998), and amended with formulations of N dependent C and N mineralization rates. N can
 21 both trigger the decomposition of “light” organic matter and stabilize C in “heavy” organic
 22 matter in LM3V-N. Sustained positive effect of available N on litter decomposition relies on
 23 the persistence of microbial N limitation during decomposition, which is implemented through
 24 the combination of available N supply to microbial organisms and their respiration rate. Further,
 25 LM3V-N incorporates the negative effects of N on recalcitrant organic matter decomposition
 26 through increasing the fraction of C and N fluxes into the recalcitrant pool. Formation of a slow
 27 decomposable organic matter pool leads to immobilization of ammonium and nitrate to satisfy
 28 the fixed carbon to nitrogen ratio of this pool.

29 **2.1.1.3 Competing sinks of available N**

1 The fate of soil mineral N (i.e. ammonium and nitrate) depends on the relative strength of the
 2 competing sinks, with the broad hierarchy of sorption > soil immobilization > plant uptake >
 3 leaching/denitrification. Denitrification thus far has been lumped with leaching losses and
 4 summed into a generic N loss term. Sorption/desorption buffers available N and is assumed to
 5 have the highest priority and be at steady state in each model time step. N immobilization into
 6 organic matter occurs during transfers among litter and soil organic matter pools. Leaching
 7 losses of available N are simulated on the basis of drainage rate. Plant uptake of mineral N is a
 8 combination of both active and passive processes. The active uptake is modeled as a Monod
 9 function, and the passive transport is a function of available N and plant transpiration.

$$10 \quad U_{N,P,pot,i} = \frac{v_{max}C_r N_{i,av}}{h_s(k_{p,1/2} + [N_{av}])} + [N_{av}]Q_{W,T} \quad (4)$$

11 where v_{max} ($\text{yr}^{-1} \text{kgC}^{-1}$) stands for the maximum uptake rate per unit root mass C_r , h_s is soil depth,
 12 $k_{p,1/2}$ is the half saturation constant, and $Q_{W,T}$ represents the transpiration flux of water. Potential
 13 uptake and thus effective removal of available N occurs if plants are N limited (see Equation
 14 3).

15 **2.1.1.4 N losses from organic pools**

16 Over the long term, N losses via fire and DON are critical factors limiting ecosystem N
 17 accumulation and maintaining N limitation in LM3V-N (Gerber et al., 2010; Thomas et al.,
 18 2015). N volatilized from fire is approximated as a function of C released from fire,
 19 stoichiometric ratio of burned tissues and reduced by a global retention factor representing the
 20 fraction of N that is retained as ash (*ash_fraction*, currently set as 0.45). DON leaching is linked
 21 to hydrologic losses of dissolved organic matter (L_{DOM}) and its C:N ratio. In turn L_{DOM} is based
 22 on drainage rate ($Q_{W,D}$) and a buffer or sorption parameter b_{DOM} (currently set as 20).

$$23 \quad L_{DOM} = \frac{Q_{W,D}}{h_s b_{DOM}} DOM \quad (5)$$

24 where DOM is the amount of dissolve organic matter in the soil column. Soil depth (h_s) is used
 25 to convert DOM unit to concentration (in unit of kgC m^{-3}). Production of DOM (in unit of kgC
 26 m^{-2}) is assumed to be proportional to the decomposition flux of the structural litter and soil
 27 water content. Both, losses via fire and via DOM are losses from a plant-unavailable pool
 28 (Thomas et al., 2015), and have the potential to increase or maintain N limitation over longer
 29 timescales, and consequently reduce N available for N_2O production through sustained and
 30 strong plant N uptake (see Equations 2-4).

1 **2.1.1.5 Biological nitrogen fixation (BNF)**

2 BNF in LM3V-N is dynamically simulated on the basis of plant N availability, N demand and
3 light condition. BNF increases if plant N requirements are not met by uptake. The rate of up-
4 regulation is swift for tropical trees but constrained by light penetrating the canopy for other
5 PFTs, mimicking the higher light requirements for new recruits that possibly can convert
6 atmospheric N₂ into plant available forms. In turn, sufficient N uptake reduces BNF. The BNF
7 parameterization thus creates a negative feedback, where high plant available N and thus the
8 potential for denitrification is counteracted with reduction of N input into the plant-soil system.
9 This explicit negative feedback is different to other models where BNF is parameterized based
10 on NPP (Thornton et al., 2007), or transpiration (Zaehle and Friend, 2010).

11 **2.1.2 Soil N₂O emission**

12 LM3V-N assumes that nitrification is linearly scaled to ammonium content, and modified by
13 soil temperature and soil moisture. Gaseous losses so far were not differentiated from
14 hydrological leaching. We add a soil nitrification-denitrification module which accounts for N
15 gaseous losses from NH₃ volatilization, nitrification and denitrification. The nitrification-
16 denitrification scheme implemented here combines features from both the DNDC model (Li et
17 al., 1992;Li et al., 2000) and the CENTURY/DAYCENT (Parton et al., 1996;Parton et al.,
18 2001;Del Grosso et al., 2000). In this part, we provide details on the nitrification-denitrification
19 module which explicitly simulates N gaseous losses from nitrification and denitrification, as
20 well as other process modifications compared to the original LM3V-N.

21 **2.1.2.1 Nitrification-Denitrification**

22 Transformation among mineral N species (ammonium and nitrate) occurs mainly through two
23 microbial pathways: nitrification and denitrification. Although ongoing debate exists in whether
24 nitrification rates may be well described by bulk soil ammonium concentration or soil N
25 turnover rate (Parton et al., 1996;Zaehle and Dalmonech, 2011), we adopt the donor controlled
26 scheme (ammonium concentration). In addition to substrate, soil texture, soil water filled pore
27 space (WFPS, the fraction of soil pore space filled with water), and soil temperature are all well
28 known regulators of nitrification. As a first order approximation, nitrification rate (N , in unit,
29 kgN m⁻² year⁻¹) is simulated as a function of soil temperature, NH₄⁺ availability and WFPS,

$$1 \quad N = k_n f_n(T) f_n(WFPS) \frac{N_{NH_4^+}}{b_{N,NH_4^+}}$$

2 (6)

3 where k_n is the optimum nitrification rate (11000 year⁻¹, the same as in LM3V-N) (Gerber et al.,
 4 2010); $N_{NH_4^+}$ is ammonium content (in unit, kgN m⁻²); b_{N,NH_4^+} is the buffer or sorption
 5 parameter for NH₄⁺ (unitless, 10 in LM3V-N) (Gerber et al., 2010); $f_n(T)$ is the temperature
 6 response function following Li et al. (2000), with an optimum temperature for nitrification at
 7 35°C; and $f_n(WFPS)$ is the soil water response function. The effect of WFPS on nitrification is
 8 texture dependent, with most of the reported optimum value around 0.6 (Parton et al., 1996; Linn
 9 and Doran, 1984). We adopt the empirical WFPS response function from Parton et al. (1996)
 10 with medium soil texture.

$$11 \quad f_n(T) = \left(\frac{60-T_{soil}}{25.78}\right)^{3.503} \times e^{\frac{3.503 \times (T_{soil}-34.22)}{25.78}} \quad (7)$$

$$12 \quad f_n(WFPS) = \left(\frac{WFPS-1.27}{-0.67}\right)^{\frac{1.9028}{0.59988}} \times \left(\frac{WFPS-0.0012}{0.59988}\right)^{2.84} \quad (8)$$

13 where T_{soil} is the soil temperature in degree Celsius.

14 Denitrification is controlled by substrate NO₃⁻ (electron acceptor), labile C availability (electron
 15 donor), soil moisture and temperature. Labile C availability is estimated by soil heterotrophic
 16 respiration (HR). Following LPJ-DyN (Xu-Ri and Prentice, 2008), denitrification is assumed
 17 to have a Q₁₀ value of 2 when the soil temperature is between 15 and 25 °C. The soil moisture
 18 response function is adopted from Parton et al. (1996). Soil pH is reported to be an important
 19 indicator of chemodenitrification which occurs predominantly in acidic soils (pH<5) under
 20 conditions of high nitrite concentration (Li et al., 2000). However, its role for N₂O production
 21 is not well studied (Li et al., 2000) and we do not model the chemodenitrification explicitly.

$$22 \quad D = k_d f_d(T) f_d(WFPS) f_g NO_3^- \quad (9)$$

$$23 \quad \text{And } f_g = \frac{HR}{HR+K_C} \frac{NO_3^-}{NO_3^-+K_n} \quad (10)$$

$$24 \quad NO_3^- = \frac{N_{NO_3^-}}{b_{NO_3^-}} \quad (11)$$

25 where D is the denitrification rate (in unit, kgN m⁻² year⁻¹); k_d is the optimum denitrification
 26 rate (8750 year⁻¹); f_g mimics the impact of labile C availability and substrate (nitrate) on the
 27 growth of denitrifiers, adapted from Li et al. (2000); K_c and K_n are half-saturation constants

1 taken from Li et al. (2000) (0.0017 and 0.0083 kgN m⁻² respectively, assuming an effective soil
 2 depth of 0.1m); $b_{NO_3^-}$ is the buffer or sorption parameter for NO₃⁻ (unitless, 1 in LM3V-N)
 3 (Gerber et al., 2010); $N_{NO_3^-}$ and NO_3^- are nitrate content before and after being buffered (in unit,
 4 kgN m⁻²), respectively; and $f_d(T)$ and $f_d(WFPS)$ are empirical soil temperature and water reponse
 5 function for denitrification, adopted from Xu-Ri and Prentice (2008) and Parton et al. (1996),
 6 respectively.

$$7 \quad f_d(T) = e^{308.56 \times (\frac{1}{68.02} + \frac{1}{T_{soil} + 46.02})} \quad (12)$$

$$8 \quad f_d(WFPS) = \frac{1.56}{12.0 \cdot (\frac{16.0}{12.0(2.01 \times WFPS)})} \quad (13)$$

9 **2.1.2.2 Gaseous partitions from nitrification-denitrification**

10 N₂O is released as a byproduct from both nitrification and denitrification. The fraction of N₂O
 11 lost from net nitrification is uncertain (Li et al., 2000; Xu-Ri and Prentice, 2008). Here we set
 12 this fraction to be 0.4%, which is higher than Goodroad and Keeney (1984), but at the low end
 13 provided by Khalil et al. (2004). N₂O and NO_x emissions from nitrification are based on the
 14 NO_x: N₂O ratio ($R_{NO_x:N_2O}$) which is updated at every time step and for each grid cell. $R_{NO_x:N_2O}$
 15 varies with relative gas diffusivity (D_r , the relative gas diffusivity in soil compared to air)
 16 (Parton et al., 2001), which is calculated from air filled porosity ($AFPS$, i.e., the portion of soil
 17 pore space that is filled by air) (Davidson and Trumbore, 1995)

$$18 \quad R_{NO_x:N_2O} = 15.2 + \frac{35.5 \times ATAN(0.68 \times \pi \times (10 \times D_r - 1.68))}{\pi} \quad (14)$$

$$19 \quad D_r = 0.209 \times AFPS^{\frac{4}{3}} \quad (15)$$

20 where ATAN stands for the trigonometric arctangent function; $AFPS$ is the air filled porosity
 21 (1-WFPS), and π is the mathematical constant, approximately 3.14159.

22 During denitrification, the gaseous ratio between N₂ and N₂O ($R_{N_2:N_2O}$) is calculated following
 23 the empirical function derived by Del Grosso et al. (2000), which combines the effects of
 24 substrate (NO₃⁻) to electron donor (HR , the proxy for labile C) ratio and WFPS. $R_{N_2:N_2O}$ is
 25 updated at every time step and for each grid cell.

$$26 \quad R_{N_2:N_2O} = Fr(\frac{NO_3^-}{HR}) \cdot Fr(WFPS) \quad (16)$$

27 With

$$Fr\left(\frac{NO_3^-}{HR}\right) = \max(0.16 \times k, k \times e^{(-0.8 \times \frac{NO_3^-}{HR})}) \quad (17)$$

$$Fr(WFPS) = \max(0.1, 0.015 \times WFPS - 0.32) \quad (18)$$

where k is a texture dependent parameter (Table 1) estimated from Del Grosso et al. (2000). k controls the maximum value of the function $Fr\left(\frac{NO_3^-}{HR}\right)$.

2.1.2.3 Other modified processes

To complete the N loss scheme in LM3V-N, we also added NH_3 volatilization into LM3V-N. NH_3 volatilization in soil results from the difference between the equilibrium NH_3 partial pressure in soil solution and that in the air. Dissolved NH_3 is regulated by ammonium concentration and pH. The net flux of NH_3 from soil to the atmosphere varies with soil NH_3 , moisture, temperature, therefore

$$NH_3 = k_{nh} f(pH) f_{NH_3}(T) (1 - WFPS) \frac{N_{NH_4^+}}{b_{N, NH_4^+}} \quad (19)$$

where NH_3 is the net ammonia volatilization flux (in unit, $kgN\ m^{-2}\ year^{-1}$); k_{nh} is the optimum ammonia volatilization rate ($365\ year^{-1}$); $f(pH)$ is the pH factor and $f(T)$ is the temperature factor which are given by the following two equations:

$$f(pH) = e^{2 \times (pH_{soil} - 10)} \quad (20)$$

$$f_{NH_3}(T) = \min(1, e^{308.56 \times (\frac{1}{71.02} - \frac{1}{T_{soil} + 46.02})}) \quad (21)$$

where pH_{soil} is the soil pH which is prescribed instead of simulated dynamically. $f(pH)$ and $f(T)$ follow largely on the NH_3 volatilization scheme implemented in the dynamic global vegetation model LPJ-DyN (Xu-Ri and Prentice, 2008).

2.2 Model experiments

2.2.1 Global hindcast with potential vegetation

To understand the model performance and compare with other models and observations, we conducted a hindcast simulation with potential vegetation. The model resolution was set to 3.75 degrees longitude by 2.5 degrees latitude. We forced the model with 3 hourly reanalysis weather data based on Sheffield et al. (2006). We used a 17 year recycled climate of 1948-1964 for the spin-up and simulation years prior to 1948. Atmospheric CO_2 concentration was prescribed with 284 ppm for model spin-up and based on ice core and atmospheric measurements for

1 transient simulations (Keeling et al., 2009). N deposition was set as natural background for
2 simulations before 1850 (Dentener and Crutzen, 1994), and interpolated linearly between the
3 natural background and a snapshot of contemporary (1995) deposition (Dentener et al., 2006)
4 for simulations after 1850. Soil pH was prescribed and derived from the Harmonized World
5 Soil Database (HWSD) version 1.1, the same as NACP model driver data (Wei et al., 2014).

6 The model was spun up from bare ground without C-N interactions for the first 68 years and
7 with C-N interactions for the following 1200 years to develop and equilibrate C and N stocks.
8 To speedup the spin-up process, slow litter and soil C and N pools were set to the equilibrium
9 values based on litterfall inputs and decomposition/leaching rates every 17 years. We
10 determined the model to reach a quasi-equilibrium state by confirming the drift to be less than
11 0.03 PgC yr^{-1} for global C storage and 0.2 TgN yr^{-1} for global N storage. From this quasi
12 equilibrium state, we initialized the global hindcast experiment starting from 1850 using the
13 corresponding climatic forcings, CO_2 and N deposition data. In the following analysis, we will
14 focus mostly on the last three decades (1970-2005).

15 **2.2.2 Sensitivity to soil water filled pore space (WFPS)**

16 While LM3V-N carries a simplified hydrology, we bracketed effects of soil moisture by
17 exploring the parameterization of WFPS and by substituting the predicted soil moisture with 3-
18 hourly re-analysis data. Levels of soil water (in unit kg m^{-2}) therefore stem from: (1) the
19 simulated water content based on LM3V-N soil water module, hereafter LM3V-SM (2) the
20 Global Land Data Assimilation System Version 2 with the land surface model NOAH 3.3
21 (Rodell et al., 2004), hereafter NOAH-SM, and (3) the ERA Interim reanalysis dataset from
22 European Center for Medium range Weather Forecasting (ECMWF) (Dee et al., 2011),
23 hereafter ERA-SM. The latter two datasets integrate satellite and ground based observations with
24 land surface models. When overriding soil moisture, we linearly interpolated the 3 hourly data
25 onto the 30 minutes model time step. In these simulations, we allowed soil C and N dynamics
26 to vary according to different soil moisture datasets, but kept the model prediction of soil water
27 to use for plant productivity and evapotranspiration.

28 Parameterization of the soil moisture effect on nitrification and denitrification are based on
29 WFPS. LM3V-N uses the concept of plant available water, where water that is available to
30 plants varies between the wilting point and field capacity. Water content above the available
31 water capacity (i.e., the difference between field capacity and wilting point) leaves the soil

1 immediately (Milly and Shmakin, 2002), and thus WFPS does not attain high values typically
2 observed during denitrification. To explore the effect of WFPS – soil moisture relationship on
3 N₂O emissions, we calculated WFPS using three methods. Method 1 assumes WFPS is the ratio
4 of available water and the available water capacity in the rooting zone. In Method 2 we assume,
5 WFPS is the ratio of the water filled porosity and total porosity which is derived from bulk
6 density (BD, in unit g cm⁻³). BD was obtained from the Harmonized World Soil Database
7 (HWSD) version 1.1 (Wei et al., 2014). The calculation is given by

$$8 \quad WFPS = \frac{\frac{\theta}{\rho h_r}}{1 - \frac{BD}{PD}} \quad (22)$$

9 where θ (kg m⁻²) is the root zone soil water; h_r (m) is the effective rooting depth of vegetation;
10 ρ is the density of water (1000 kg m⁻³); and PD is the particle density of soil (2650 kg m⁻³).
11 Method 1 geerally leads to an overestimation of WFPS because the available water capacity
12 smaller than total pore space. In contrast, the use of Method 2 with LM3V-SM creates an
13 underestimation since water is not allowed to accumulate beyond field capacity and misses high
14 WFPS to which nitrification and denitrification are sensitive. Meanwhile, for NOAH-SM and
15 ERA-SM data, Methods 2 is more close to the “real” WFPS and is the default method when
16 using these data sets. In a third approach, which is also the default method with LM3V-SM that
17 is applied in the global hindcast experiment, the subsequent elevated CO₂ and temperature
18 responses experiment, and sensitivity tests with regard to N cycling, calculates WFPS as the
19 average of the previous two methods.

20 For each soil moisture dataset (3 in total, 2 replacements and 1 simulated by LM3V-N), we
21 calculated WFPS using three methods mentioned above. We conducted transient simulations
22 with the nine different WFPSs (3 datasets × 3 methods) starting from the near equilibrium state
23 obtained in the global hindcast experiment in 2.2.1. The use of less realistic Method for WFPS
24 for each soil moisture driver (LM3V-SM, NOAH-SM and ERA-SM) offers insights of the
25 sensitivity of N₂O emissions to soil moisture. The simulation procedure was the same as that
26 in global hindcast experiment except for the WFPS. ERA-SM is only availabe starting from
27 1979, prior to which simulations were conducted with model default soil moisture (LM3V-SM).
28 Results from ERA-SM were analyzed starting from 1982, leaving a short period for adjustment.

1 **2.2.3 Sensitivity to N cycling processes and parameterization**

2 N₂O emission is constraint by ecosystem availability of mineral N, which is linked to different
3 N cycling processes in addition to nitrification and denitrification processes. To test the
4 sensitivity of modelled N₂O emission to the larger plant-soil N cycle, we conducted the
5 following sensitivity analyses, in form of a one at a time perturbation. We replaced the dynamic
6 BNF scheme with empirically reconstructed preindustrial fixation rates (Cleveland et al., 1999),
7 removing the negative feedback between BNF and plant N availability. We further shut off N
8 loss pathways through DON leaching and fire volatilization (with *ash_fraction* =1). We expect
9 that these three modifications alleviate N limitation: Prescribed BNF may continuously add N
10 beyond plant N demand. Further eliminating fire and DOM N losses leave loss pathways that
11 have to pass the available N pool thereby opening the possibility of increasing gaseous losses.
12 Further, removing these plant-unavailable pathways (Thomas et al., 2015) increases N retention
13 and opens the possibility of alleviating N limitation. In addition, we modified key parameters
14 related to general N cycling and N₂O emissions one-at-a-time. We multiplied several
15 parameters that directly affect ammonium and nitrate concentration or N₂O fluxes by 10 (x10)
16 or 0.1 (x0.1), while kept other parameters as defaults. Those parameters control the active root
17 N uptake rates (v_{max}), nitrification rate (k_n), denitrification rate (k_d, K_c, K_n) and the fraction of
18 net nitrification lost as N₂O (*frac*),

19 **2.2.4 Responses to elevated CO₂ and temperature**

20 Responses of N₂O emissions to atmospheric CO₂ and global warming have been reported at field
21 scale (Dijkstra et al., 2012; van Groenigen et al., 2011). Here, we evaluate the model's response
22 to step changes in form of a doubling of preindustrial CO₂ level (284 ppm to 568 ppm) and a
23 2K increase in atmospheric temperature. Starting from the same quasi-equilibrium state with
24 potential vegetation as in the global hindcast experiment in 2.2.1, we conducted four transient
25 model runs: (1) the CONTROL run with the same drivers as spin-up; (2) the CO₂_FERT run
26 with the same drivers as the CONTROL except a doubling of atmospheric CO₂ level; (3) the
27 TEMP run with the same drivers as the CONTROL except a 2K rise in atmospheric temperature;
28 and (4) the CO₂_FERT×TEMP run with both the doubling of CO₂ and 2K rise in temperature.
29 For each experiment, we ran the model for 100 years and evaluated the corresponding results.

1 **2.3 Comparisons with observations**

2 We compared our model results for annual N₂O gas loss with field data: We compiled annual
3 N₂O emissions from peer-reviewed literature (see Appendix A for more information). To
4 increase the representativeness of the measurements, we included only sites with more than 3
5 months or 100 days experimental span. We limited our datasets where there was no reference
6 to a disturbance of any kind. Only locations with at least 50 years non-disturbance history for
7 forests and 10 years for vegetation other than forests were included. The compiled 61
8 measurements cover a variety of spatial ranges with vegetation types including tropical
9 rainforest, temperate forest, boreal forest, tundra, savanna, perennial grass, steppe, alpine grass
10 and desert vegetation. Multiple measurements falling into the same model grid cell were
11 averaged. If the authors had indicated the dominant vegetation or soil type, we used the values
12 reported for the dominant type instead of the averaged. For multiyear measurements, even if
13 the authors gave the individual year's data, we averaged the data to avoid overweighting of long
14 term studies. If the location was between borders of different model grid cells, we averaged
15 across the neighboring grid cells.

16 We also compared monthly N₂O fluxes at a group of sites: (a) the Tapajós National Forest in
17 Amazonia (3°S, 55°W), taken from Davidson et al. (2008); (b) the Hubbard Brook
18 Experimental Forest in New Hampshire, USA (44°N, 72°W), as described in Groffman et al.
19 (2006); (c) the cedar forest from Oita, Japan (33°N, 131°E), as described in Morishita et al.
20 (2007); (d) the *Leymus chinensis* (LC) and *Stipa grandis* (SG) steppe in Inner Mongolia, China
21 (44°N, 117°E), taken from Xu-Ri et al. (2003); (e) the cedar forest in Fukushima, Japan (37°N,
22 140°E), taken from Morishita et al. (2007); and (f) the primary (P1 and P2) and secondary (L1
23 and L2) forests located at the Pasir Mayang Research Site (1°S, 102°E), Indonesia, taken from
24 Ishizuka et al. (2002). In addition, daily measurements of soil temperature, soil moisture and
25 N₂O emissions were compared at four German forest sites located in the same grid cell (50°N,
26 8°E), as described in Schmidt et al. (1986).

27 **3 Results**

28 **3.1 Global budget, seasonal and inter-annual variability**

29 Our modelled global soil N₂O flux is 6.69±0.32 TgN yr⁻¹ (1970-2005 mean and standard
30 deviation among different years) (Fig.1) with LM3V-SM (Method 3, default method for

1 LM3V-N calculated soil moisture), 5.61 ± 0.32 TgN yr⁻¹ with NOAH-SM (Method 2) and
2 7.47 ± 0.30 TgN yr⁻¹ with ERA-SM (1982-2005, Method 2) which is within the range of reported
3 values: The central estimation of N₂O emission from soils under natural vegetation is 6.6 TgN
4 yr⁻¹ based on the Intergovernmental Panel on Climate Change (IPCC) AR5 (Ciais et al., 2013)
5 (range, 3.3–9.0 TgN yr⁻¹) for the mid-1990s. Mean estimation for the period of 1975-2000
6 ranged from 7.4 to 10.6 TgN yr⁻¹ with different precipitation forcing data (Saikawa et al., 2013).
7 Xu-Ri et al. (2012) reported the decadal-average to be 8.3-10.3 TgN yr⁻¹ for the 20th century.
8 Potter and Klooster (1998) reported a global mean emission rate of 9.7 TgN yr⁻¹ over 1983-
9 1988, which is higher than the earlier version of their model (6.1 TgN yr⁻¹) (Potter et al., 1996).
10 Other estimates includes 6-7 TgN yr⁻¹ (Syakila and Kroeze, 2011), 6.8 TgN yr⁻¹ based on the
11 O-CN model (Zaehle et al., 2011), 3.9-6.5 TgN yr⁻¹ for preindustrial periods from a top-down
12 inversion study (Hirsch et al., 2006), 1.96-4.56 TgN yr⁻¹ in 2000 extrapolated from field
13 measurements by an artificial neural network approach (Zhuang et al., 2012), 6.6-7.0 TgN yr⁻¹
14 for 1990 (Bouwman et al., 1995), and 7-16 TgN yr⁻¹ (Bowden, 1986) as well as 3-25 TgN yr⁻¹
15 (Banin, 1986) from two earlier studies.

16 Following Thompson et al. (2014), El Niño years are set to the years with the annual
17 multivariate ENSO index (MEI) greater than 0.6. 1972, 1977, 1982, 1983, 1987, 1991, 1992,
18 1993, 1994, 1997 and 1998 were chosen as El Niño years. We detected reduced emissions
19 during El Niño years (Fig. 1), in line with the global atmospheric inversion study of Thompson
20 et al. (2014) and the process based modelling study from Saikawa et al. (2013).

21 Figure 2 shows the simulated global natural soil N₂O emissions in 4 seasons averaged over the
22 period of 1970-2005 based on LM3V-SM (Method 3). The northern hemisphere displays a large
23 seasonal variability, with the highest emissions in the northern summer (JJA, June to August)
24 and lowest in winter (DJF, December to February). Globally, northern spring (MAM, March to
25 May) has the highest emission rate (2.07 TgN) followed by summer (1.89 TgN). The smaller
26 emissions in summer compared to spring stems from a reduced contribution of the southern
27 hemisphere during northern summer.

28 As expected, a large portion (more than 60%) of the soil N₂O fluxes have tropical origin (23.5
29 S to 23.5N), while emissions from cooler regions are limited by temperature and arid/semi-arid
30 regions by soil water. Our modelling results suggested year-round high emission rates from
31 humid zones of Amazonia, east central Africa, and throughout the islands of Southeast Asia,
32 with small seasonal variations (Fig. 2). Emissions from tropical savannah are highly variable,

1 with locations of both high fluxes (seasonal mean $> 30 \text{ mgN m}^{-2} \text{ month}^{-1}$ or $3.6 \text{ kg ha}^{-1} \text{ yr}^{-1}$) and
2 low fluxes (seasonal mean $< 1.3 \text{ mgN m}^{-2} \text{ month}^{-1}$ or $0.16 \text{ kg ha}^{-1} \text{ yr}^{-1}$). The simulated average
3 tropical emission rate is $0.78 \text{ kgN ha}^{-1} \text{ yr}^{-1}$ (1970-2005), within the range of estimates ($0.2\text{-}1.4$
4 $\text{kgN ha}^{-1} \text{ yr}^{-1}$) based on site-level observations from the database of Stehfest and Bouwman
5 (2006), but smaller than a more detailed simulation study ($1.2 \text{ kgN ha}^{-1} \text{ yr}^{-1}$) carried out by
6 Werner et al. (2007). Our analysis here excluded land cover, land use changes and human
7 management impacts, while most of the observation-based or regional modelling studies did
8 not factor out those impacts. Our modelling result in natural tropics is comparable with another
9 global modelling study (average emission rate, $0.7 \text{ kgN ha}^{-1} \text{ yr}^{-1}$) (Zaehle et al., 2010), in which
10 the authors claimed they may underestimate the tropical N_2O sources compared to the inversion
11 estimates from the atmospheric transport model TM3 (Hirsch et al., 2006).

12 **3.2 Sensitivity to WFPS**

13 The different parameterization of WFPS and the use of different soil moisture modeling and
14 data allows to test the sensitivity of soil N_2O emissions to variable WFPS. Globally, emissions
15 generally increase with WFPS (Fig. 3). WFPS derived from Method 1 is higher than that based
16 on Method 2. Data-derived soil moisture datasets combined with different calculation methods
17 together produced a range of $0.15\text{-}0.72$ for the global mean WFPS (1982-2005). While mean
18 values greater than 0.6 (approximately field capacity) are less realistic, these high WFPS values
19 provide the opportunity to test the model's response to the soil moisture-based parameterization
20 of redox conditions in soils. Global soil N_2O emissions are highly sensitive to WFPS, with
21 approximately 0.25 TgN per year per 0.01 change in global mean WFPS in the range 0 to 0.6 .
22 The spatial and temporal characteristic of WFPS also matters. Emission rate from LM3V-SM
23 (Fig. 3 green cycle) is 1.13 TgN yr^{-1} higher than that from NOAH-SM (Fig. 3 blue triangle),
24 while both model configuration have the same mean WFPS (ca 0.21), highlighting effects of
25 regional and temporal differences between the soil moisture products.

26 **3.3 Model-observation comparisons**

27 Modelled N_2O emissions capture the average of cross-site observed annual mean emissions
28 (0.54 vs. $0.53 \text{ kgN ha}^{-1} \text{ yr}^{-1}$ based on LM3V-SM) reasonably (Appendix A and Fig. 4a), but
29 spread considerably along the 1:1 line. The points deviating the most are from tropical forests,
30 with overestimations from montane tropical forest and underestimations from lowland tropical
31 forests if those measurements are representative of gridcell emissions. These patterns are

1 similar as results from NOAH-SM (Appendix A and Fig. 4b) and ERA-SM (Appendix A and
2 Fig. 4c), except that the application of WFPS from NOAH-SM slightly underestimates the
3 observed global mean (0.54 vs. 0.47 kgN ha⁻¹ yr⁻¹ from NOAH-SM with WFPS based on
4 Method 2).

5 At the Tapajós National Forest, results from LM3V-SM capture some of the variations in N₂O
6 fluxes, but the model is not able to reproduce the high emissions observed during spring (Panel
7 (a), Fig. 5). At the Hubbard Brook Experimental Forest, the correlation between model results
8 and observations are 0.51 (LM3V-SM), 0.56 (NOAH-SM) and 0.62 (ERA-SM) for yellow
9 birch, 0.66 (LM3V-SM), 0.68 (NOAH-SM) and 0.70 (ERA-SM) for sugar maple. However,
10 the model is less robust in reproducing the magnitude of emission peaks. Groffman et al. (2006)
11 suggested high emissions of N₂O in winter were associated with soil freezing. However, the
12 model assumes little emissions when soil temperature is under 0 °C. In addition, observations
13 suggested N₂O uptake (negative values in Panel (b), Fig. 5) while the model does not
14 incorporate mechanisms to represent N₂O uptake. At the Oita cedar forest, model reproduces
15 the seasonality of N₂O emissions accurately (Panel (c), Fig. 5). ERA-SM overestimates the
16 magnitude of N₂O fluxes from Inner Mongolia grassland, while the magnitudes produced from
17 LM3V-SM and NOAH-SM are comparable with observations. However, the timing of the
18 emission peaks are one or two month in advance from model output compared to observations
19 (Panel (d), Fig. 5). At the Fukushima cedar forest, similar as at the Oita cedar forest, models
20 are less robust at capturing the magnitude of high peaks despite the seasonality produced by the
21 model are good (Panel (e), Fig. 5). Emissions from the primary and secondary tropical rainforest
22 at the Pasir Mayang Research Site are highly variable, which makes the comparison difficult
23 (Panel (f), Fig. 5). LM3V-SM (but not ERA-SM and NOAH-SM) reproduces the low emissions
24 in September-November 1997 and the increase of emissions from secondary forests in
25 December, 1997. Overall, modeled variability is smaller compared to observation.

26 The strong variability of measured N₂O emissions is further illustrated in Fig. 6. Difference in
27 measured N₂O fluxes between different forest sites within one grid cell is large, reflecting the
28 heterogeneity that is not captured within one grid cell. In addition, the error bars, which
29 represent the standard deviation of measured N₂O fluxes at three different plots of the same
30 forest, are large. The standard deviation is as high as 49.27 µgN m⁻²h⁻¹, indicating the strong
31 variability of measured N₂O fluxes at the plot scale. Modeled N₂O fluxes are generally within

1 the range of measured N₂O emissions. Model outputs slightly underestimate N₂O emissions
2 largely due to the underestimation of soil water content (Panel (b) Fig. 6).

3 **3.4 Sensitivity to N cycling processes and parameterization**

4 Disallowing of N losses through DON and fire volatilization enhance ecosystem N
5 accumulation and availability to plants and microbes, and therefore increases N₂O emissions
6 (Panel (a), Fig.7). The gain in N₂O emissions from disallowing DON loss is small (0.12 TgN
7 yr⁻¹). However, N₂O emission is on average (1950-2005) increased by 3.63 TgN yr⁻¹ in the
8 absence of fire volatilization N loss (we note, that fires do occur, but N is retained as ash in the
9 litter). The gain is most evident in tropical regions (not shown), indicating the importance of
10 fire in regulating ecosystem N status. Simulated preindustrial BNF is smaller than the empirical
11 reconstructed BNF (72 in LM3V-N vs. 108 TgN yr⁻¹ from empirical based data). However,
12 BNF in LM3V-N increases with time under historical varying climate, increasing atmospheric
13 CO₂ level and N deposition. The global average BNF during 1950-2005 is 100 TgN yr⁻¹, close
14 to the empirical value. Nevertheless, substitution of BNF in LM3V-N by empirical preindustrial
15 value increased N₂O flux by 1.2 TgN yr⁻¹(Panel (a), Fig.7).

16 Among the specific parameters tested, N₂O emission is most sensitive to the 10 times change
17 (x10) of the fraction of net nitrification lost as N₂O gas. The relative magnitude of N₂O flux on
18 average (1950-2005) reaches 6.5 times of the default (Panel (b), Fig.7). Reduction (x0.1) of
19 maximum active plant N uptake strength (v_{max}) strongly increases N₂O emissions (*ca.* by 3 times
20 of the default). Meanwhile, enhancement of v_{max} also increases N₂O fluxes, reflecting the non-
21 linear response of N₂O emissions to v_{max} . x10 in the maximum nitrification rate k_n and
22 denitrification rate k_d increase N₂O emissions, while x0.1 decrease N₂O flux. N₂O increases
23 more with increasing k_d than with increasing k_n , whereas reduction of k_n (x0.1) produces a
24 stronger response than reduction of k_d . The half-saturation constant that represents the
25 regulation of labile carbon availability on denitrification rate, K_c , is the least sensitive parameter.
26 Meanwhile, reduction (x0.1) of the half-saturation constant K_n that represents the regulation of
27 substrate availability on denitrification rate on average increased N₂O fluxes by 4.5 TgN yr⁻¹
28 ¹(Panel (b), Fig.7).

1 3.5 CO₂ and temperature responses

2 Globally, N₂O emissions respond to a step CO₂ increase first with a decline to ultimately
3 increased levels after approximately 40 years (Fig. 8a, black line). The simulated global
4 response follows largely the behaviour as simulated for tropical forests (Fig. 8a, yellow line).
5 The shift from a negative to a positive response indicates possible competing mechanisms
6 operating on different time scales. Field level experiments revealed the highly variable effects
7 of CO₂ fertilization on N₂O emissions. Based on a meta-analysis, van Groenigen et al. (2011)
8 suggested that elevated CO₂ significantly increased N₂O emission by 18.8%, while Dijkstra et
9 al. (2012) argued for a non-significant response in non-N-fertilized studies. In contrast to
10 observation studies, the global C-N cycle model analyses from O-CN suggested negative CO₂
11 fertilization effects on N₂O emissions (Zaehle et al., 2011). The negative impacts (reduced N₂O
12 flux), which are also reported in manipulative experiments, are likely from increased plant N
13 and immobilization demand under CO₂ fertilization, reducing N availability for nitrifiers and
14 denitrifiers (Dijkstra et al., 2012). CO₂ fertilization on average (over 100 years) increased the
15 global mean plant nitrogen uptake rate by 10.02 kgN ha⁻¹ yr⁻¹, as shown in Fig. 9 (Panel (b)).
16 Modelled soil inorganic N content (ammonium and nitrate) is reduced at first, but the reduction
17 is not sustained. One mechanism to alleviate CO₂ fertilization caused N limitation is through
18 BNF, which is on average (over 100 years) more than doubled (Fig. 9 Panel (e)). Similar as
19 manipulative field experiments (Dijkstra et al., 2012), positive effects (increase N₂O fluxes)
20 can result from the impacts of elevated CO₂ level to increase litter production (Fig. 9 Panel (a))
21 and consequently C sources for denitrifiers, and to increase soil moisture (Fig. 9 Panel (d)) from
22 reduced stomatal conductance and leaf transpiration (Fig. 9 Panel (c)). With both positive and
23 negative mechanisms embedded in our model, the net effects depend on the relative strength of
24 the opposing forces.

25 Temperate deciduous forests, where most of the forest CO₂ fertilization experiments are
26 conducted, respond positively to elevated CO₂ level (Fig. 8a, green line). The slight increase in
27 modelled N₂O emission are comparable with the mean response of field data compiled for
28 temperate forests (*ca.* 0.01-0.03 kgN yr⁻¹ ha⁻¹) (Dijkstra et al., 2012). A similar positive response
29 was detected for cold evergreen forests (Fig. 8a, pink line) with stronger magnitude compared
30 to temperate deciduous forests. For grasslands, Dijkstra et al. (2012) reported small negative
31 mean response from northern mixed prairie (Δ N₂O, *ca.* -0.01 to -0.03 kgN yr⁻¹ ha⁻¹), zero mean
32 response from shortgrass steppe and positive mean response from annual grassland (*ca.* 0.03-

1 0.06 kgN yr⁻¹ ha⁻¹). Our model shows a small negative mean response from C4 grassland (Fig.
2 8a, cyan line) with the similar magnitude of that reported for the Northern mixed prairie, where
3 the composition of C4 grass varies (Dijkstra et al., 2012). A CO₂ increase in C3 grassland
4 initially reduces N₂O emission (Fig. 8a, blue line). However, this slight negative response turns
5 into a small positive within one decade.

6 Elevated temperature generally increases N₂O emissions except for the slight negative effect in
7 C4 grass (Fig. 8b). Overall the response to a 2 degree warming is bigger than that of doubling
8 of CO₂. The simulated temperature effects are more pronounced in the first decade and decrease
9 over time in tropical forests (Fig. 8b, yellow line), while for the temperate deciduous forests
10 (Fig. 8b, green line) and boreal forests (Fig.8b pink line), the temperature effects become more
11 pronounced over time. Simulated temperate forest response (in the first decade) is close to that
12 of observed mean (*ca.* 0.2-0.5 kgN yr⁻¹ ha⁻¹) (Dijkstra et al., 2012). Our modelled slight negative
13 response in C4 grass and positive in C3 grass are in alignment with data compiled by Dijkstra
14 et al. (2012) who reported both positive and negative responses in grasslands.

15 The results of combining CO₂ and temperature are similar to the CO₂ effect alone (Fig. 8c),
16 despite the fact, that the individual effect of temperature is much stronger than that of CO₂. This
17 antagonistic interaction (i.e. the combined enhancement in N₂O flux from elevated CO₂ and
18 temperature are smaller than the summary of their individual effects) is also evident for C3
19 grass (first 50 years), temperate deciduous tree and cold evergreen forests (Fig. 8d).

20 **4 Discussion**

21 Our model combines two of the most widely applied biogeochemical models (DNDC and
22 CENTURY) with current advancements in field level studies. The model is capable of
23 reproducing the global mean natural N₂O emissions from other modeling and inverse methods,
24 and the average of observed cross-site annual mean behavior. By focusing on the role of soil
25 moisture in N₂O emissions, we find a global scale high dependence of simulated N₂O emissions
26 on soil moisture (WFPS), mainly driven by emissions from tropical regions. The model broadly
27 reproduces the magnitude and direction of responses to elevated CO₂ and temperature from
28 manipulative field experiments where data is available. The global responses to elevated CO₂
29 and temperature follow largely the response of tropical forests, where a noted absence of field
30 experiments exist.

31 Evaluation of global simulations against field measurements is susceptible to scale mismatches.
32 The complexity of microscale interactions for N₂O production creates notorious large spatial

1 and temporal variabilities which are undoubtedly difficult to constraint even at the stand level
2 (Butterbach-Bahl et al., 2013). Daily measurements from the German forest sites (Fig.6)
3 illustrate the large variability in N₂O emissions. Further improvement in soil moisture
4 simulation will improve our estimation of N₂O fluxes at the German forest sites. However, the
5 homogeneous representation of environmental drivers within model grid cells casts doubt on
6 site-specific model-observation comparison in global simulations. For example, N₂O emissions
7 vary with topography which are not treated explicitly in most of the global C-N models. 3.8
8 times difference was detected in a montane forest (Central Sulawesi, Indonesia) moving from
9 1190 m to 1800m (Purbopuspito et al., 2006), and 4.3 times difference was found from a tropical
10 moist forest (Brazilian Atlantic Forest) with the altitude change from 100m to 1000m (Sousa
11 Neto et al., 2011). However, comparison against field data revealed, that the model's variability
12 is smaller compared to observation for both across field sites (Fig. 4), and at different sites (Figs.
13 5 and 6). One of the reason for this shortcoming may be that fast transitions, such as freeze-
14 thaw cycle (Groffman et al., 2006) and pulsing (Yienger and Levy, 1995) are not sufficiently
15 captured.

16 Soil moisture is a key variable in climate system but difficult to derive or measure at the global
17 scale (Seneviratne et al., 2010). Our modelled fluxes are highly sensitive to WFPS, which is in
18 agreement with observation and model synthesis studies (Heinen, 2006; Butterbach-Bahl et al.,
19 2013). The large range when calculating WFPS from different methods resulted in a difference
20 of more than 5 TgN yr⁻¹ in global soil N₂O fluxes. Saikawa et al. (2013) found an up to 3.5 TgN
21 yr⁻¹ gap induced by different precipitation forcing data from CLMCN-N₂O. It is difficult to
22 single out the difference caused by soil moisture alone from their results. Nevertheless, those
23 two studies did suggest the importance of improving the dynamics of soil water and
24 representation of WFPS for the purpose of predicting soil N₂O emission and climate feedbacks.

25 The root zone soil water in LM3V-N is based on a single layer bucket model. This simplified
26 treatment of soil water dynamics may increase the difficulty in reproducing the temporal and
27 spatial dynamics of WFPS. As a first step, we used the average between the original analog in
28 LM3V-N and that is derived from soil total porosity to account for actual soil moisture and the
29 possibility of soil water above field capacity. Meanwhile, overriding soil moisture with data-
30 derived products (NOAH-SM and ERA-SM), suggests that the most realistic average (1970-
31 2005) soil N₂O emission is in the range of 5.61-7.47 TgN yr⁻¹. A more realistic root zone water
32 module, such as multilayer representations of biogeochemistry and soil water dynamics, would

1 refine models of soil N₂O emissions. El Niño events trigger reduced soil emissions in our results
2 similar as proposed by Saikawa et al. (2013) and Thompson et al. (2014). El Niño events are
3 known to have induced several of the most well known large scale droughts and alters soil
4 moisture dynamics (Schwalm et al., 2011). Tropical forests N₂O emissions are highly correlated
5 with root zone soil water content and contribute strongly to the global-scale fluxes of N₂O in
6 our model. Whether there is a strong link between soil N₂O emission anomalies and El Niño
7 induced soil moisture deviations needs further investigation with improved soil hydrology.

8 Globally, the tropical fluxes contribute with more than 60% to the global soil N₂O fluxes. Also,
9 global responses to elevated CO₂ and temperature are dominated by the tropical response. In
10 contrast to temperate and boreal forests, tropical forests respond negatively to elevated CO₂ in
11 the first few decades. Our results therefore suggest caution when extrapolating from current
12 manipulative field studies to the globe: The positive response to CO₂ enrichment as obtained
13 from (mostly) extratropical field study may be overestimated, when the studies' fluxes are
14 scaled up to the globe. Moreover, we found strong interaction of elevated CO₂ and temperature,
15 acting to reduce soil N₂O emission compared to the sum of individual responses, highlighting
16 the non-linear impacts of CO₂ and temperature on N₂O emissions. Our results from step
17 increases of CO₂ and temperature is different from Xu-Ri et al. (2012) in which CO₂ and climate
18 change act synergistically to increase historical N₂O emissions, especially in tropical regions.
19 CO₂ fertilization plus interaction with temperature rise reduce tropical N₂O fluxes in the first
20 several decades from our model. We realize that this interaction is likely to be different when
21 incorporating other factors (Brown et al., 2012), such as N deposition, precipitation and land
22 use change (disturbance). In addition, step changes in atmospheric CO₂ and temperature
23 compared to gradual and sustained increases may also lead to differences, and may explain the
24 discrepancy between the previous modeling study and meta-analysis of manipulative field
25 experiments with regard to CO₂ fertilization responses (Zaehle et al., 2011; van Groenigen et
26 al., 2011). However, step changes mimic most closely manipulative experiments. Nevertheless,
27 the largest uncertainties lie in the tropical region where our model indicated strongest responses
28 and strongest nonlinear interactions of elevated CO₂ and temperature.

29 Globally, N₂O emissions from nitrification-denitrification are similar to O-CN and LPJ-DyN
30 as they are all derived from DNDC. Embedding an established N₂O emission module into
31 LM3V-N enables evaluation of the response of N₂O emissions under different assumptions
32 across models with respect to the dynamics of the larger plant-soil N cycle. Generally higher

1 inputs from BNF or constraints on losses through organic N (fire, DON) enhance N₂O
2 emissions. The representation of of BNF in models requires improvement but we show here that
3 different implementations are globally important for N₂O emissions. Similar, the magnitude of
4 N lost through fire impacts N₂O emissions in fire prone regions, while N emission factors are
5 poorly constrained globally (Andreae and Merlet, 2001). The strength of plant uptake of N
6 poses a strong constraint on the availability of N for nitrification-denitrification losses as it can
7 draw down N substantially (Gerber and Brookshire, 2014). A reduction of plant uptake strength
8 allows for relatively more N allocated for denitrification. More surprising was the positive
9 effect of a stronger plant uptake capacity on N₂O emissions: Enhanced plant uptake allow
10 increased vegetation production, and an throughput through litterfall and mineralization in the
11 long run, which ultimately may allow higher N₂O losses in lieu of other export pathways. In
12 addition to those N cycling processes N₂O emission is highly sensitive to the fraction of N lost
13 as N₂O from net nitrification. The fraction of N₂O lost from net nitrification is uncertain.
14 Goodroad and Keeney (1984) suggested a value of 0.1-0.2% , while Khalil et al. (2004) reported
15 a range of 0.16%-1.48% depending on the O₂ concentration. We applied a global constant of
16 0.4% in our default simulation, bearing in mind the large uncertainties associated with this
17 parameter. We also note that this value has significant impact on global N₂O emissions.

18 The response to increases in temperature and CO₂ is a consequence of both the direct effect of
19 temperature on nitrification and denitrification, and indirect effects via water and mineral N
20 availability. The initial negative response of N₂O emissions to CO₂ fertilization from tropical
21 forests produced by LM3V-N stems largely from the increased demand and uptake of mineral
22 N due to enhanced vegetation growth under elevated atmospheric CO₂ level. Despite soil N
23 availability has been reported to decrease, unchanged or increase from manipulative CO₂
24 enrichment experiments across extrotropical ecosystems (Reich et al., 2006; Drake et al., 2011;
25 Reich and Hobbie, 2013), no empirical evidence is available in tropical forests. LM3V-N
26 produced, on average, a reduced soil mineral N concentration in tropical forests initially.
27 Consequently, less N is available for gaseous losses. If gross mineralization is used as an
28 indicator of the rate of N flow in the “hole-in-the-pipe” concept and gaseous losses are
29 proportional to mineralization, the initial negative response is unlikely to be detected. We found
30 increased mineralization rate with increased litterfall under elevated CO₂, while N availability
31 is reduced from LM3V-N. The mineralization based approach is likely to predict an increase of
32 losses regardless of N limitation. In LM3V-N, N availability recovers as N cycling processes

1 adjust to CO₂ fertilization, especially from BNF, but also via higher transient retention of N
2 from deposition.

3 In addition to the uncertainties mentioned above, we simplified N₂O sources and processes,
4 ignoring other microbial metabolic pathways and abiotic processes that produce or consume
5 N₂O. The global magnitude of those ignored process remains largely unexplored. We do not
6 incorporate explicit mechanisms for N₂O emissions from freeze-thaw cycle or poorly drained
7 soils (e.g. wetlands), the uptake of organic N etc., which are be globally important, especially
8 with future climate changes. Considering those uncertainties and gaps, more studies are in need
9 in order to understand the terrestrial N₂O emissions.

10 **5 Conclusions**

11 We present estimates of terrestrial soil N₂O fluxes under natural vegetation (1970 to 2005)
12 based on existing N₂O emission formulations embedded into the global C-N cycle model
13 LM3V-N. To determine the sensitivity of the modelling result to soil water (WFPS), we
14 replaced the root zone soil water with two other derived datasets and altered the way in which
15 WFPS is calculated. Our best estimate of modelled global soil N₂O flux is 5.61-7.47 TgN yr⁻¹
16 (1970-2005 mean and interannual variability), within the range of current understanding of soil
17 N₂O emissions, but highly sensitive to WFPS, general N cycling and parameterization of N₂O
18 losses through nitrification and denitrification. Improvement of soil hydrology is likely to
19 significantly reduce the large uncertainties associated with soil N₂O emission estimates.
20 Although the simulated mean responses are in agreement with manipulative field studies where
21 effects of elevated CO₂ and temperature were investigated, we found that the global response
22 was dominated by tropical forest, where our model suggest a different response than the field
23 studies carried out in temperate ecosystems.

24

1

2 **Appendix A: Observed annual N₂O fluxes data**

3 Annual N₂O fluxes data were compiled from peer-reviewed literature. We applied simple
 4 selection criteria (see the main text) to reduce the mismatches between model outputs and field
 5 measurements, bearing in mind the gaps between complex field conditions and idealized model
 6 forcings. Latitudes (Lat) and longitudes (Lon) in Table A1 are based on model grids.

7 **Table A1 Observed annual N₂O emission data for model comparison**

No	Country	Lon	Lat	Location	Veg Type	N ₂ O kgN ha ⁻¹ yr ⁻¹			
						OBS	LM3V-N	NOAH	ERA
1	Australia	133.1	-12.3	Douglas Daly region	Savanna	0.02	0.15	0.25	
2	Australia	148.1	-37.3	Moe	Temperate forest	0.11	0.58	0.74	0.72
3	Australia	151.9	-27.3	South-east Queensland	Tropical forest	0.52	0.01	0.03	
4	Austria	16.9	47.8	Klausenleopoldsdorf	Temperate forest	0.62	0.64	0.52	0.53
5	Austria	9.4	47.8	Achenkirch	Temperate forest	0.35	0.54	0.48	0.47
6	Austria	13.1	47.8	Innsbruck	Temperate forest	0.08	0.42	0.36	0.31
7	Austria	16.3	48.2	Schottenwald and Klausenleopoldsdorf	Temperate forest	0.76	0.61	0.54	0.53
8	Brazil	-61.9	-2.3	Manaus	Tropical rain forest	1.9	1.6	1.68	1.56
9	Brazil	-61.9	-2.3	Manaus	Tropical rain forest	1.930	1.71	1.74	1.55
10	Brazil	-54.4	-4.8	East-central Amazonia	Tropical rain forest	2.1	1.34	2.19	1.57
11	Brazil	-46.9	-2.3	Paragominas	Rainforest	2.430	1.22	1.19	1.11
12	Burkina Faso	-1.9	10.3	Ioba	Savanna	0.6	0.03	1.32	
13	Canada	-80.6	50.3	Ontario	Boreal forest	0.04	0.11	0.14	0.12
14	Canada	-106.9	52.8	Saskatchewan	Boreal forest	0.28	0.01	0.01	0.01
15	Canada	-103.1	52.8	Saskatchewan	Boreal forest	0.07	0.21	0.17	
16	Canada	-106.9	52.8	Saskatchewan	Boreal forest	0.09	0.01	0.01	
17	Canada	-73.1	45.3	Mont St. Hilaire	Temperate forest	0.42	0.54	0.46	
18	China	91.9	35.3	Tibet	Alpine grassland	0.07	0	0	0
19	China	125.6	40.3	Changbai mountain	Alpine tundra, temperate forest	0.56	0.73	0.64	0.45
20	China	114.4	42.8	Inner mongolia	Temperate forest	0.73	0.1	0.14	0.71
22	China	133.1	47.8	Sanjiang Experimental Station	Freshwater marshes	0.21	0.34	0.35	0.34

23	Denmark	13.1	55.3	Solo	Temperate forest	0.29	0.27	0.42	0.06
24	Denmark	13.1	55.3	Denmark	Temperate forest	0.52	0.28	0.37	0.05
25	Ecuador	-80.6	-4.8	Bombuscaro	Tropical forest	0.3	1.02	0	
26	Finland	24.4	60.3	Southern	Boreal forest	0.78	0.62	0.35	0.17
27	Germany	9.4	50.3	Average	Temperate forest	0.57	0.6	0.53	0.5
28	Germany	9.4	52.8	Kiel	Temperate forest	0.4	0.48	0.53	0.52
29	Germany	9.4	47.8	Southwest	Temperate forest	0.93	0.56	0.51	0.49
30	Germany	13.1	47.8	Höglwald	Temperate forest	0.41	0.47	0.4	0.39
31	Germany	9.4	52.8	Average	Temperate forest	0.66	0.44	0.5	0.5
32	Germany	9.4	52.8	Harz mountains	Mire	0.25	0.48	0.56	0.52
34	Indonesia	103.1	-2.3	Jambi	Lowland tropical rainforest	0.260	0.44		
35	Indonesia	121.9	-2.3	Central Sulawesi	Tropical seasonal rain forest	0.800	1.73	2.31	1.7
36	Indonesia	114.4	-2.3	Central Kalimantan	Tropical forest	2.51	2	2.45	1.73
37	Italy	9.4	45.3	P.Ticino BoscoNegri	Temperate forest	0.18	1.38	2.8	1.82
38	Malaysia	110.6	-2.3	Sarawak	Mixed peat swamp forest	0.7	0.66	0.65	0.57
39	New Zealand	170.6	-44.8	New Zealand	Temperate forest	0.01	1.24	2.84	1.24
40	Norway	9.4	60.3	Norway	Temperate forest	0.73	0.52	0.52	0.38
41	Panama	-80.6	7.8	Gigante Peninsula	Tropical forests	1.6	0.2	0.39	0.39
42	Sweden	13.1	57.8	Southwestern	Temperate forest	0.07	1.86	1.67	
43	Sweden	13.1	57.8	Asa experimental forest	Undrained bog	0.65	0.36	0.45	0.36
44	UK	-1.9	55.3	Northumberland	Grassland	0.3	0.4	0.5	0.41
45	USA	-73.1	42.8	Harvard forest	Mixed hardwood	0.04	0.56	0.54	0.48
46	USA	-73.1	40.3	New York	Temperate forest	0.9	0.4	0.49	0.41
47	USA	-80.6	25.3	Florida	Marsh	1	0.45	0	
48	USA	-73.1	42.8	New Hampshire	Temperate forest	0.070	0.64	2.15	
49	USA	-106.9	35.3	New mexico	Temperate forest	0.06	0.41	0.51	0.43
50	USA	-118.1	45.3	Washington	Temperate shrub-steppe	0.15	0.02	0.02	0.02
51	USA	-114.4	37.8	Mojave desert	Perennial grasses	0.11	0.02	0.02	0.02
52	USA	-106.9	40.3	Wyoming	Sagebrush steppe	0.21	0.01	0.02	0.03
53	USA	-73.1	45.3	Northeastern	Temperate forest	0.18	0.05	0.04	0.05
54	USA	-69.4	45.3	Northeastern	Temperate forest	0.03	0.53	0.46	0.44
55	USA	-103.1	40.3	Colorado	Temperate steppe	0.14	0.37	0.53	0.4
56	USA	-88.1	42.8	Wisconsin	Grass	0.040	0.03	0.05	0.05
57	USA	-114.4	37.8	Nevada	Mojave desert	0.11	0.45	0.45	

58	USA	-110.6	32.8	Arizona	Sonoran desert	0.4	0.04	0.04	0.05
59	USA	-118.1	45.3	Ft. Collins, Colorado	Temperate grassland	0.12	0.01	0.03	0.03
60	Venezuela	-61.9	10.3	Venezuela	Savana	0.73	0.06	0.07	0.07
61	Zimbabwe	31.9	-17.3	Harare	Miombo woodland savanna	0.51	0.83	1.61	0.57

1

2 References cited in the Appendix

- 3 Ball, T., Smith, K. A., and Moncrieff, J. B.: Effect of stand age on greenhouse gas fluxes from
4 a Sitka spruce [*Picea sitchensis* (Bong.) Carr.] chronosequence on a peaty gley soil, *Global*
5 *Change Biol.*, 13, 2128-2142, doi:10.1111/j.1365-2486.2007.01427.x, 2007.
- 6 Billings, S. A., Schaeffer, S. M., and Evans, R. D.: Trace N gas losses and N mineralization in
7 Mojave desert soils exposed to elevated CO₂, *Soil Biol. Biochem.*, 34, 1777-1784,
8 doi:10.1016/s0038-0717(02)00166-9, 2002.
- 9 Bowden, R. D., Steudler, P. A., Melillo, J. M., and Aber, J. D.: Annual nitrous-oxide fluxes
10 from temperate forest soils in the northeastern United-States, *J. Geophys. Res.-Atmos.*, 95,
11 13997-14005, doi:10.1029/JD095iD09p13997, 1990.
- 12 Bruemmer, C., Brueggemann, N., Butterbach-Bahl, K., Falk, U., Szarzynski, J., Vielhauer, K.,
13 Wassmann, R., and Papen, H.: Soil-atmosphere exchange of N₂O and NO in near-natural
14 savanna and agricultural land in Burkina Faso (W. Africa), *Ecosystems*, 11, 582-600,
15 doi:10.1007/s10021-008-9144-1, 2008.
- 16 Brumme, R., Borken, W., and Finke, S.: Hierarchical control on nitrous oxide emission in forest
17 ecosystems, *Glob. Biogeochem. Cycles*, 13, 1137-1148, doi:10.1029/1999gb900017, 1999.
- 18 Castro, M. S., Steudler, P. A., Melillo, J. M., Aber, J. D., and Millham, S.: Exchange of N₂O
19 and CH₄ between the atmosphere and soils in spruce-fir forests in the northeastern United-
20 States, *Biogeochemistry*, 18, 119-135, doi:10.1007/bf00003273, 1992.
- 21 Cates, R. L., Jr., and Keeney, D. R.: Nitrous oxide emission from native and reestablished
22 prairies in southern Wisconsin, *American Midland Naturalist*, 117, 35-42, 1987.
- 23 Chen, G. X., Huang, B., Xu, H., Zhang, Y., Huang, G. H., Yu, K. W., Hou, A. X., Du, R., Han,
24 S. J., and VanCleemput, O.: Nitrous oxide emissions from terrestrial ecosystems in China,
25 *Chemosphere: Global Change Science*, 2, 373-378, 2000.
- 26 Davidson, E. A., Nepstad, D. C., Ishida, F. Y., and Brando, P. M.: Effects of an experimental
27 drought and recovery on soil emissions of carbon dioxide, methane, nitrous oxide, and nitric
28 oxide in a moist tropical forest, *Global Change Biol.*, 14, 2582-2590, doi:10.1111/j.1365-
29 2486.2008.01694.x, 2008.
- 30 Du, R., Lu, D., and Wang, G.: Diurnal, seasonal, and inter-annual variations of N₂O fluxes from
31 native semi-arid grassland soils of inner mongolia, *Soil Biol. Biochem.*, 38, 3474-3482,
32 doi:10.1016/j.soilbio.2006.06.012, 2006.
- 33 Duxbury, J. M., Bouldin, D. R., Terry, R. E., and Tate, R. L.: Emissions of nitrous-oxide from
34 soils, *Nature*, 298, 462-464, doi:10.1038/298462a0, 1982.

- 1 Groffman, P. M., Hardy, J. P., Driscoll, C. T., and Fahey, T. J.: Snow depth, soil freezing, and
2 fluxes of carbon dioxide, nitrous oxide and methane in a northern hardwood forest, *Global*
3 *Change Biol.*, 12, 1748-1760, doi:10.1111/j.1365-2486.2006.01194.x, 2006.
- 4 Grover, S. P. P., Livesley, S. J., Hutley, L. B., Jamali, H., Fest, B., Beringer, J., Butterbach-
5 Bahl, K., and Arndt, S. K.: Land use change and the impact on greenhouse gas exchange in
6 north Australian savanna soils, *Biogeosciences*, 9, 423-437, doi:10.5194/bg-9-423-2012, 2012.
- 7 Guilbault, M. R., and Matthias, A. D.: Emissions of N₂O from Sonoran Desert and effluent-
8 irrigated grass ecosystems, *J. Arid Environ.*, 38, 87-98, doi:10.1006/jare.1997.0300, 1998.
- 9 Henrich, M., and Haselwandter, K.: Denitrification and gaseous nitrogen losses from an acid
10 spruce forest soil, *Soil Biol. Biochem.*, 29, 1529-1537, doi:10.1016/s0038-0717(97)00010-2,
11 1997.
- 12 Ishizuka, S., Tsuruta, H., and Murdiyarso, D.: An intensive field study on CO₂, CH₄, and N₂O
13 emissions from soils at four land-use types in Sumatra, Indonesia, *Global Biogeochem. Cycles*,
14 16, GB1049, doi:10.1029/2001gb001614, 2002.
- 15 Jungkunst, H. F., Fiedler, S., and Stahr, K.: N₂O emissions of a mature Norway spruce (*Picea*
16 *abies*) stand in the black forest (southwest Germany) as differentiated by the soil pattern, *J.*
17 *Geophys. Res.-Atmos.*, 109, D07302, doi:10.1029/2003jd004344, 2004.
- 18 Keller, M., Kaplan, W. A., and Wofsy, S. C.: Emissions of N₂O, CH₄ and CO₂ from tropical
19 forest soils, *J. Geophys. Res.-Atmos.*, 91, 1791-1802, doi:10.1029/JD091iD11p11791, 1986.
- 20 Kesik, M., Ambus, P., Baritz, R., Bruggemann, N. B., Butterbach-Bahl, K., Damm, M., Duyzer,
21 J., Horvath, L., Kiese, R., Kitzler, B., Leip, A., Li, C., Pihlatie, M., Pilegaard, K., Seufert, G.,
22 Simpson, D., Skiba, U., Smiatek, G., Vesala, T., and Zechmeister-Boltenstern, S.: Inventories
23 of N₂O and NO emissions from European forest soils, *Biogeosciences*, 2, 353-375, 2005.
- 24 Khalil, M. A. K., Rasmussen, R. A., French, J. R. J., and Holt, J. A.: The influence of termites
25 on atmospheric trace gases: CH₄, CO₂, CHCl₃, N₂O, CO, H₂, and light-hydrocarbons, *J.*
26 *Geophys. Res.-Atmos.*, 95, 3619-3634, doi:10.1029/JD095iD04p03619, 1990.
- 27 Kitzler, B., Zechmeister-Boltenstern, S., Holtermann, C., Skiba, U., and Butterbach-Bahl, K.:
28 Nitrogen oxides emission from two beech forests subjected to different nitrogen loads,
29 *Biogeosciences*, 3, 293-310, 2006.
- 30 Klemedtsson, L., Klemedtsson, A. K., Moldan, F., and Weslien, P.: Nitrous oxide emission
31 from Swedish forest soils in relation to liming and simulated increased N-deposition, *Biol. Fert.*
32 *Soil.*, 25, 290-295, doi:10.1007/s003740050317, 1997.
- 33 Koehler, B., Corre, M. D., Veldkamp, E., Wullaert, H., and Wright, S. J.: Immediate and long-
34 term nitrogen oxide emissions from tropical forest soils exposed to elevated nitrogen input,
35 *Global Change Biol.*, 15, 2049-2066, doi:10.1111/j.1365-2486.2008.01826.x, 2009.
- 36 Luizao, F., Matson, P., Livingston, G., Luizao, R., and Vitousek, P.: Nitrous oxide flux
37 following tropical land clearing, *Glob. Biogeochem. Cycles*, 3, 281-285,
38 doi:10.1029/GB003i003p00281, 1989.
- 39 Luo, G. J., Bruggemann, N., Wolf, B., Gasche, R., Grote, R., and Butterbach-Bahl, K.: Decadal
40 variability of soil CO₂, NO, N₂O, and CH₄ fluxes at the Höglwald Forest, Germany,
41 *Biogeosciences*, 9, 1741-1763, doi:10.5194/bg-9-1741-2012, 2012.

- 1 Maljanen, M., Jokinen, H., Saari, A., Strommer, R., and Martikainen, P. J.: Methane and nitrous
2 oxide fluxes, and carbon dioxide production in boreal forest soil fertilized with wood ash and
3 nitrogen, *Soil Use Manage.*, 22, 151-157, doi:10.1111/j.1475-2743.2006.00029.x, 2006.
- 4 Matson, A., Pennock, D., and Bedard-Haughn, A.: Methane and nitrous oxide emissions from
5 mature forest stands in the boreal forest, Saskatchewan, Canada, *Forest Ecol. Manag.*, 258,
6 1073-1083, doi:10.1016/j.foreco.2009.05.034, 2009.
- 7 Matson, P. A., Volkman, C., Coppinger, K., and Reiners, W. A.: Annual nitrous-oxide flux
8 and soil-nitrogen characteristics in sagebrush steppe ecosystems, *Biogeochemistry*, 14, 1-12,
9 1991.
- 10 Matson, P. A., Gower, S. T., Volkman, C., Billow, C., and Grier, C. C.: Soil nitrogen cycling
11 and nitrous oxide flux in a Rocky Mountain Douglas-fir forest: effects of fertilization, irrigation
12 and carbon addition, *Biogeochemistry*, 18, 101-117, doi:10.1007/bf00002705, 1992.
- 13 Melling, L., Hatano, R., and Goh, K. J.: Nitrous oxide emissions from three ecosystems in
14 tropical peatland of Sarawak, Malaysia, *Soil Sci. Plant Nutr.*, 53, 792-805, doi:10.1111/j.1747-
15 0765.2007.00196.x, 2007.
- 16 Mogge, B., Kaiser, E. A., and Munch, J. C.: Nitrous oxide emissions and denitrification N-
17 losses from forest soils in the Bornhöved Lake region (Northern Germany), *Soil Biol.*
18 *Biochem.*, 30, 703-710, doi:10.1016/s0038-0717(97)00205-8, 1998.
- 19 Mosier, A. R., Parton, W. J., Valentine, D. W., Ojima, D. S., Schimel, D. S., and Delgado, J.
20 A.: CH₄ and N₂O fluxes in the Colorado shortgrass steppe .1. Impact of landscape and nitrogen
21 addition, *Glob. Biogeochem. Cycles*, 10, 387-399, doi:10.1029/96gb01454, 1996.
- 22 Mummey, D. L., Smith, J. L., and Bolton, H.: Small-scale spatial and temporal variability of
23 N₂O flux from a shrub-steppe ecosystem, *Soil Biol. Biochem.*, 29, 1699-1706,
24 doi:10.1016/s0038-0717(97)00077-1, 1997.
- 25 Parton, W. J., Mosier, A. R., and Schimel, D. S.: Rates and pathways of nitrous-oxide
26 production in a shortgrass steppe, *Biogeochemistry*, 6, 45-58, 1988.
- 27 Pei, Z. Y.: Carbon dynamics in the alpine grassland ecosystem on the tibetan plateau—a case
28 study of wudaoliang, qinghai province, PhD thesis, Institute of Geographic Sciences and
29 Natural Resources Research, Beijing, China, 2003.
- 30 Price, S. J., Sherlock, R. R., Kelliher, F. M., McSeveny, T. M., Tate, K. R., and Condron, L.
31 M.: Pristine new zealand forest soil is a strong methane sink, *Global Change Biol.*, 10, 16-26,
32 doi:10.1046/j.1529-8817.2003.00710x, 2004.
- 33 Purbopuspito, J., Veldkamp, E., Brumme, R., and Murdiyarso, D.: Trace gas fluxes and
34 nitrogen cycling along an elevation sequence of tropical montane forests in Central Sulawesi,
35 Indonesia, *Glob. Biogeochem. Cycles*, 20, GB3010, doi:10.1029/2005gb002516, 2006.
- 36 Rees, R. M., Wuta, M., Furley, P. A., and Li, C. S.: Nitrous oxide fluxes from savanna
37 (miombo) woodlands in Zimbabwe, *J. Biogeogr.*, 33, 424-437, 2005.
- 38 Rowlings, D. W., Grace, P. R., Kiese, R., and Weier, K. L.: Environmental factors controlling
39 temporal and spatial variability in the soil-atmosphere exchange of CO₂, CH₄ and N₂O from an
40 Australian subtropical rainforest, *Global Change Biol.*, 18, 726-738, doi:10.1111/j.1365-
41 2486.2011.02563.x, 2012.

- 1 Schiller, C. L., and Hastie, D. R.: Nitrous oxide and methane fluxes from perturbed and
2 unperturbed boreal forest sites in northern Ontario, *J. Geophys. Res.-Atmos.*, 101, 22767-
3 22774, doi:10.1029/96jd01620, 1996.
- 4 Simona, C., Ariangelo, D. P. R., John, G., Nina, N., Ruben, M., and Jose, S. J.: Nitrous oxide
5 and methane fluxes from soils of the Orinoco savanna under different land uses, *Global Change*
6 *Biol.*, 10, 1947-1960, doi:10.1111/j.1365-2486.2004.00871.x, 2004.
- 7 Simpson, I. J., Edwards, G. C., Thurtell, G. W., den Hartog, G., Neumann, H. H., and Staebler,
8 R. M.: Micrometeorological measurements of methane and nitrous oxide exchange above a
9 boreal aspen forest, *J. Geophys. Res.-Atmos.*, 102, 29331-29341, doi:10.1029/97jd03181,
10 1997.
- 11 Sitaula, B. K., Bakken, L. R., and Abrahamsen, G.: N-fertilization and soil acidification effects
12 on N₂O and CO₂ emission from temperate pine forest soil, *Soil Biol. Biochem.*, 27, 1401-1408,
13 doi:10.1016/0038-0717(95)00078-s, 1995.
- 14 Struwe, S., and Kjoller, A.: Field determination of denitrification in water-logged forest soils,
15 *FEMS Microbiol. Ecol.*, 62, 71-78, 1989.
- 16 Takakai, F., Morishita, T., Hashidoko, Y., Darung, U., Kuramochi, K., Dohong, S., Limin, S.
17 H., and Hatano, R.: Effects of agricultural land-use change and forest fire on N₂O emission
18 from tropical peatlands, Central Kalimantan, Indonesia, *Soil Sci. Plant Nutr.*, 52, 662-674,
19 doi:10.1111/j.1747-0765.2006.00084.x, 2006.
- 20 Tauchnitz, N., Brumme, R., Bernsdorf, S., and Meissner, R.: Nitrous oxide and methane fluxes
21 of a pristine slope mire in the German National Park Harz Mountains, *Plant and Soil*, 303, 131-
22 138, doi:10.1007/s11104-007-9493-0, 2008.
- 23 Templer, P. H., Mack, M. C., Chapin, F. S., III, Christenson, L. M., Compton, J. E., Crook, H.
24 D., Currie, W. S., Curtis, C. J., Dail, D. B., D'Antonio, C. M., Emmett, B. A., Epstein, H. E.,
25 Goodale, C. L., Gundersen, P., Hobbie, S. E., Holland, K., Hooper, D. U., Hungate, B. A.,
26 Lamontagne, S., Nadelhoffer, K. J., Osenberg, C. W., Perakis, S. S., Schleppei, P., Schimel, J.,
27 Schmidt, I. K., Sommerkorn, M., Spoelstra, J., Tietema, A., Wessel, W. W., and Zak, D. R.:
28 Sinks for nitrogen inputs in terrestrial ecosystems: A meta-analysis of ¹⁵N tracer field studies,
29 *Ecology*, 93, 1816-1829, 2012.
- 30 Ullah, S., and Moore, T. R.: Biogeochemical controls on methane, nitrous oxide, and carbon
31 dioxide fluxes from deciduous forest soils in eastern Canada, *J. Geophys. Res.-Biogeo.*, 116,
32 GB3010, doi:10.1029/2010jg001525, 2011.
- 33 Verchot, L. V., Davidson, E. A., Cattanio, J. H., Ackerman, I. L., Erickson, H. E., and Keller,
34 M.: Land use change and biogeochemical controls of nitrogen oxide emissions from soils in
35 eastern Amazonia, *Glob. Biogeochem. Cycles*, 13, 31-46, doi:10.1029/1998gb900019, 1999.
- 36 von Arnold, K., Nilsson, M., Hanell, B., Weslien, P., and Klemedtsson, L.: Fluxes of CO₂, CH₄
37 and N₂O from drained organic soils in deciduous forests, *Soil Biol. Biochem.*, 37, 1059-1071,
38 doi:10.1016/j.soilbio.2004.11.004, 2005.
- 39 Wolf, K., Veldkamp, E., Homeier, J., and Martinson, G. O.: Nitrogen availability links forest
40 productivity, soil nitrous oxide and nitric oxide fluxes of a tropical montane forest in southern
41 Ecuador, *Glob. Biogeochem. Cycles*, 25, doi:10.1029/2010gb003876, 2011.
- 42 Yu, J., Liu, J., Wang, J., Sun, W., Patrick, W. H., Jr., and Meixner, F. X.: Nitrous oxide emission
43 from *deyeuxia angustifolia* freshwater marsh in northeast China, *Environ. Manage.*, 40, 613-
44 622, doi:10.1007/s00267-006-0349-9, 2007.
- 45

1 **Acknowledgements**

2 The Soil moisture data used in this study were acquired as part of the mission of NASA's Earth
3 Science Division and archived and distributed by the Goddard Earth Sciences (GES) Data and
4 Information Services Center (DISC). We would like to thank Lex Bouwman, Benjamin Stocker
5 and an anonymous reviewer for helpful suggestions.

6 **References**

- 7 Andreae, M. O., and Merlet, P.: Emission of trace gases and aerosols from biomass burning,
8 *Glob. Biogeochem. Cycles*, 15, 955-966, doi:10.1029/2000gb001382, 2001.
- 9 Banin, A.: Global budget of N₂O: The role of soils and their change, *Sci. Total Environ.*, 55,
10 27-38, doi:10.1016/0048-9697(86)90166-x, 1986.
- 11 Bolker, B. M., Pacala, S. W., and Parton, W. J.: Linear analysis of soil decomposition: Insights
12 from the century model, *Ecol. Appl.*, 8, 425-439, doi:10.2307/2641082, 1998.
- 13 Bouwman, A. F., Vanderhoek, K. W., and Olivier, J. G. J.: Uncertainties in the global source
14 distribution of nitrous oxide, *J. Geophys. Res.-Atmos.*, 100, 2785-2800, doi:10.1029/94jd02946,
15 1995.
- 16 Bowden, W. B.: Gaseous nitrogen emissions from undisturbed terrestrial ecosystems: An
17 assessment of their impacts on local and global nitrogen budgets, *Biogeochemistry*, 2, 249-279,
18 doi:10.1007/bf02180161, 1986.
- 19 Braker, G., and Conrad, R.: Diversity, structure, and size of N₂O-producing microbial
20 communities in soils-what matters for their functioning?, in: *Advances in Applied*
21 *Microbiology*, Vol 75, edited by: Laskin, A. I., Sariaslani, S., and Gadd, G. M., *Advances in*
22 *Applied Microbiology*, 33-70, 2011.
- 23 Brown, J. R., Blankinship, J. C., Niboyet, A., van Groenigen, K. J., Dijkstra, P., Le Roux, X.,
24 Leadley, P. W., and Hungate, B. A.: Effects of multiple global change treatments on soil N₂O
25 fluxes, *Biogeochemistry*, 109, 85-100, doi:10.1007/s10533-011-9655-2, 2012.
- 26 Butterbach-Bahl, K., Baggs, E. M., Dannenmann, M., Kiese, R., and Zechmeister-Boltenstern,
27 S.: Nitrous oxide emissions from soils: how well do we understand the processes and their
28 controls?, *Philosophical Transactions of the Royal Society B-Biological Sciences*, 368,
29 20130122–20130122, doi:10.1098/rstb.2013.0122, 2013.
- 30 Ciais, P., Sabine, C., Bala, G., Bopp, L., Brovkin, V., Canadell, J., Chhabra, A., DeFries, R.,
31 Galloway, J., Heimann, M., Jones, C., Quéré, C. L., Myneni, R. B., Piao, S., and Thornton, P.:
32 Carbon and Other Biogeochemical Cycles, in: *Climate Change 2013: The Physical Science*
33 *Basis. Contribution of Working Group I to the Fifth Assessment Report of the*
34 *Intergovernmental Panel on Climate Change*, edited by: Stocker, T. F., Qin, D., Plattner, G.-K.,
35 Tignor, M., Allen, S. K., Boschung, J., Nauels, A., Xia, Y., Bex, V., and Midgley, P. M.,
36 Cambridge University Press, Cambridge, United Kingdom and New York, NY, USA, 2013.
- 37 Cleveland, C. C., Townsend, A. R., Schimel, D. S., Fisher, H., Howarth, R. W., Hedin, L. O.,
38 Perakis, S. S., Latty, E. F., Von Fischer, J. C., Elseroad, A., and Wasson, M. F.: Global patterns
39 of terrestrial biological nitrogen (N₂) fixation in natural ecosystems, *Global Biogeochemical*
40 *Cycles*, 13, 623-645, 10.1029/1999gb900014, 1999.

- 1 Collatz, G. J., Ball, J. T., Grivet, C., and Berry, J. A.: Physiological and environmental
2 regulation of stomatal conductance, photosynthesis and transpiration: a model that includes a
3 laminar boundary layer, *Agr. Forest Meteorol.*, 54, 107-136, doi:10.1016/0168-
4 1923(91)90002-8, 1991.
- 5 Collatz, G. J., Ribas-Carbo, M., and Berry, J. A.: Coupled photosynthesis-stomatal conductance
6 model for leaves of C4 plants, *Aust. J. Plant Physiol.*, 19, 519-538, 1992.
- 7 Davidson, E. A., and Trumbore, S. E.: Gas diffusivity and production of CO₂ in deep soils of
8 the eastern Amazon, *Tellus Series B-Chemical and Physical Meteorology*, 47, 550-565,
9 doi:10.1034/j.1600-0889.47.issue5.3.x, 1995.
- 10 Davidson, E. A., Nepstad, D. C., Ishida, F. Y., and Brando, P. M.: Effects of an experimental
11 drought and recovery on soil emissions of carbon dioxide, methane, nitrous oxide, and nitric
12 oxide in a moist tropical forest, *Global Change Biology*, 14, 2582-2590, 10.1111/j.1365-
13 2486.2008.01694.x, 2008.
- 14 Davidson, E. A.: The contribution of manure and fertilizer nitrogen to atmospheric nitrous oxide
15 since 1860, *Nature Geoscience*, 2, 659-662, doi:10.1038/ngeo608, 2009.
- 16 Dee, D. P., Uppala, S. M., Simmons, A. J., Berrisford, P., Poli, P., Kobayashi, S., Andrae, U.,
17 Balmaseda, M. A., Balsamo, G., Bauer, P., Bechtold, P., Beljaars, A. C. M., van de Berg, L.,
18 Bidlot, J., Bormann, N., Delsol, C., Dragani, R., Fuentes, M., Geer, A. J., Haimberger, L., Healy,
19 S. B., Hersbach, H., Holm, E. V., Isaksen, L., Kallberg, P., Koehler, M., Matricardi, M.,
20 McNally, A. P., Monge-Sanz, B. M., Morcrette, J. J., Park, B. K., Peubey, C., de Rosnay, P.,
21 Tavolato, C., Thepaut, J. N., and Vitart, F.: The ERA-Interim reanalysis: configuration and
22 performance of the data assimilation system, *Quarterly Journal of the Royal Meteorological
23 Society*, 137, 553-597, doi:10.1002/qj.828, 2011.
- 24 Del Grosso, S. J., Parton, W. J., Mosier, A. R., Ojima, D. S., Kulmala, A. E., and Phongpan, S.:
25 General model for N₂O and N₂ gas emissions from soils due to denitrification, *Glob.
26 Biogeochem. Cycles*, 14, 1045-1060, 2000.
- 27 Dentener, F., Drevet, J., Lamarque, J. F., Bey, I., Eickhout, B., Fiore, A. M., Hauglustaine, D.,
28 Horowitz, L. W., Krol, M., Kulshrestha, U. C., Lawrence, M., Galy-Lacaux, C., Rast, S.,
29 Shindell, D., Stevenson, D., Van Noije, T., Atherton, C., Bell, N., Bergman, D., Butler, T.,
30 Cofala, J., Collins, B., Doherty, R., Ellingsen, K., Galloway, J., Gauss, M., Montanaro, V.,
31 Mueller, J. F., Pitari, G., Rodriguez, J., Sanderson, M., Solmon, F., Strahan, S., Schultz, M.,
32 Sudo, K., Szopa, S., and Wild, O.: Nitrogen and sulfur deposition on regional and global scales:
33 A multimodel evaluation, *Global Biogeochemical Cycles*, 20,
34 doi:Gb400310.1029/2005gb002672, 2006.
- 35 Dentener, F. J., and Crutzen, P. J.: A three-dimensional model of the global ammonia cycle, *J.
36 Atmos. Chem.*, 19, 331-369, doi:10.1007/bf00694492, 1994.
- 37 Dijkstra, F. A., Prior, S. A., Runion, G. B., Torbert, H. A., Tian, H., Lu, C., and Venterea, R.
38 T.: Effects of elevated carbon dioxide and increased temperature on methane and nitrous oxide
39 fluxes: evidence from field experiments, *Frontiers in Ecology and the Environment*, 10, 520-
40 527, doi:10.1890/120059, 2012.
- 41 Drake, J. E., Gallet-Budynek, A., Hofmockel, K. S., Bernhardt, E. S., Billings, S. A., Jackson,
42 R. B., Johnsen, K. S., Lichter, J., McCarthy, H. R., McCormack, M. L., Moore, D. J. P., Oren,
43 R., Palmroth, S., Phillips, R. P., Pippen, J. S., Pritchard, S. G., Treseder, K. K., Schlesinger, W.
44 H., DeLucia, E. H., and Finzi, A. C.: Increases in the flux of carbon belowground stimulate

1 nitrogen uptake and sustain the long-term enhancement of forest productivity under elevated
2 CO₂, *Ecology Letters*, 14, 349-357, 10.1111/j.1461-0248.2011.01593.x, 2011.

3 Farquhar, G. D., Caemmerer, S. V., and Berry, J. A.: A biochemical model of photosynthetic
4 CO₂ assimilation in leaves of C₃ species, *Planta*, 149, 78-90, doi:10.1007/bf00386231, 1980.

5 Firestone, M. K., and Davidson, E. A.: Microbiological basis of NO and N₂O production and
6 consumption in soil, Exchange of trace gases between terrestrial ecosystems and the
7 atmosphere., edited by: Andreae, M. O., and Schimel, D. S., 7-21 pp., 1989.

8 Forster, P., Ramaswamy, V., Artaxo, P., Berntsen, T., Betts, R., Fahey, D. W., Haywood, J.,
9 Lean, J., Lowe, D. C., Myhre, G., Nganga, J., Prinn, R., Raga, G., Schulz, M., and Dorland, R.
10 V.: Changes in Atmospheric Constituents and in Radiative Forcing, in: *Climate Change 2007:
11 The Physical Science Basis. Contribution of Working Group I to the Fourth Assessment Report
12 of the Intergovernmental Panel on Climate Change*, edited by: Solomon, S., Qin, D., Manning,
13 M., Chen, Z., Marquis, M., Averyt, K. B., M.Tignor, and Miller, H. L., Cambridge University
14 Press, Cambridge, United Kingdom and New York, NY, USA, 2007.

15 Galloway, J. N., Aber, J. D., Erisman, J. W., Seitzinger, S. P., Howarth, R. W., Cowling, E. B.,
16 and Cosby, B. J.: The nitrogen cascade, *Bioscience*, 53, 341-356, doi:10.1641/0006-
17 3568(2003)053[0341:tnc]2.0.co;2, 2003.

18 Gerber, S., and Brookshire, E. N. J.: Scaling of physical constraints at the root-soil interface to
19 macroscopic patterns of nutrient retention in ecosystems, *Am. Nat.*, 183, 418-430,
20 doi:10.1086/674907, 2014.

21 Gerber, S., Hedin, L. O., Oppenheimer, M., Pacala, S. W., and Shevliakova, E.: Nitrogen
22 cycling and feedbacks in a global dynamic land model, *Glob. Biogeochem. Cycles*, 24,
23 doi:10.1029/2008gb003336, 2010.

24 Goodroad, L. L., and Keeney, D. R.: Nitrous oxide emission from forest, marsh, and prairie
25 ecosystems, *J. Environ. Qual.*, 13, 448-452, 1984.

26 Groffman, P. M., Hardy, J. P., Driscoll, C. T., and Fahey, T. J.: Snow depth, soil freezing, and
27 fluxes of carbon dioxide, nitrous oxide and methane in a northern hardwood forest, *Global
28 Change Biology*, 12, 1748-1760, 10.1111/j.1365-2486.2006.01194.x, 2006.

29 Heinen, M.: Simplified denitrification models: Overview and properties, *Geoderma*, 133, 444-
30 463, doi:10.1016/j.geoderma.2005.06.010, 2006.

31 Hirsch, A. I., Michalak, A. M., Bruhwiler, L. M., Peters, W., Dlugokencky, E. J., and Tans, P.
32 P.: Inverse modeling estimates of the global nitrous oxide surface flux from 1998-2001, *Glob.
33 Biogeochem. Cycles*, 20, doi:10.1029/2004gb002443, 2006.

34 Ishizuka, S., Tsuruta, H., and Murdiyarto, D.: An intensive field study on CO₂, CH₄, and N₂O
35 emissions from soils at four land-use types in Sumatra, Indonesia, *Global Biogeochemical
36 Cycles*, 16, 10.1029/2001gb001614, 2002.

37 Keeling, R. F., Piper, S. C., Bollenbacher, A. F., and Walker, J. S.: Atmospheric CO₂ records
38 from sites in the SIO air sampling network, in *Trends: A compendium of data on global change.*
39 Carbon Dioxide Information Analysis Center, Oak Ridge National Laboratory, U.S.
40 Department of Energy, Oak Ridge, Tenn., U.S.A [online] Available from:
41 <http://cdiac.ornl.gov/trends/co2/sio-mlo.html> (Accessed 13 August 2010), 2009.

42 Khalil, K., Mary, B., and Renault, P.: Nitrous oxide production by nitrification and
43 denitrification in soil aggregates as affected by O₂ concentration, *Soil Biol. Biochem.*, 36, 687-
44 699, doi:10.1016/j.soilbio.2004.01.004, 2004.

- 1 Li, C. S., Frolking, S., and Frolking, T. A.: A model of nitrous-oxide evolution from soil driven
2 by rainfall events .1. model structure and sensitivity, *J. Geophys. Res.-Atmos.*, 97, 9759-9776,
3 1992.
- 4 Li, C. S., Aber, J., Stange, F., Butterbach-Bahl, K., and Papen, H.: A process-oriented model of
5 N₂O and NO emissions from forest soils: 1. Model development, *J. Geophys. Res.-Atmos.*, 105,
6 4369-4384, doi:10.1029/1999jd900949, 2000.
- 7 Linn, D. M., and Doran, J. W.: Effect of water-filled pore space on carbon dioxide and nitrous
8 oxide production in tilled and nontilled soils, *Soil Sci. Soc. Am. J.*, 48, 1267-1272, 1984.
- 9 Milly, P. C. D., and Shmakin, A. B.: Global modeling of land water and energy balances. Part
10 I: the land dynamics (LaD) model, *J. Hydrometeorol.*, 3, 283-299, doi:10.1175/1525-
11 7541(2002)003<0283:gmolwa>2.0.co;2, 2002.
- 12 Milly, P. C. D., Malyshev, S. L., Shevliakova, E., Dunne, K. A., Findell, K. L., Gleeson, T.,
13 Liang, Z., Philipps, P., Stouffer, R. J., and Swenson, S.: An enhanced model of land water and
14 energy for global hydrologic and Earth-System studies, *J. Hydrometeorol.*, 15, 1739-1761,
15 2014.
- 16 Morishita, T., Sakata, T., Takahashi, M., Ishizuka, S., Mizoguchi, T., Inagaki, Y., Terazawa,
17 K., Sawata, S., Igarashi, M., Yasuda, H., Koyama, Y., Suzuki, Y., Toyota, N., Muro, M., Kinjo,
18 M., Yamamoto, H., Ashiya, D., Kanazawa, Y., Hashimoto, T., and Umata, H.: Methane uptake
19 and nitrous oxide emission in Japanese forest soils and their relationship to soil and vegetation
20 types, *Soil Science and Plant Nutrition*, 53, 678-691, 10.1111/j.1747-0765.2007.00181.x, 2007.
- 21 Parton, W. J., Mosier, A. R., Ojima, D. S., Valentine, D. W., Schimel, D. S., Weier, K., and
22 Kulmala, A. E.: Generalized model for N₂ and N₂O production from nitrification and
23 denitrification, *Glob. Biogeochem. Cycles*, 10, 401-412, doi:10.1029/96gb01455, 1996.
- 24 Parton, W. J., Holland, E. A., Del Grosso, S. J., Hartman, M. D., Martin, R. E., Mosier, A. R.,
25 Ojima, D. S., and Schimel, D. S.: Generalized model for NO_x and N₂O emissions from soils, *J.*
26 *Geophys. Res.-Atmos.*, 106, 17403-17419, doi:10.1029/2001jd900101, 2001.
- 27 Potter, C. S., Matson, P. A., Vitousek, P. M., and Davidson, E. A.: Process modeling of controls
28 on nitrogen trace gas emissions from soils worldwide, *J. Geophys. Res.-Atmos.*, 101, 1361-
29 1377, doi:10.1029/95jd02028, 1996.
- 30 Potter, C. S., and Klooster, S. A.: Interannual variability in soil trace gas (CO₂, N₂O, NO) fluxes
31 and analysis of controllers on regional to global scales, *Glob. Biogeochem. Cycles*, 12, 621-
32 635, doi:10.1029/98gb02425, 1998.
- 33 Purbopuspito, J., Veldkamp, E., Brumme, R., and Murdiyarso, D.: Trace gas fluxes and
34 nitrogen cycling along an elevation sequence of tropical montane forests in Central Sulawesi,
35 Indonesia, *Glob. Biogeochem. Cycles*, 20, doi:10.1029/2005gb002516, 2006.
- 36 Ravishankara, A. R., Daniel, J. S., and Portmann, R. W.: Nitrous oxide (N₂O): The dominant
37 ozone-depleting substance emitted in the 21st century, *Science*, 326, 123-125,
38 doi:10.1126/science.1176985, 2009.
- 39 Reich, P. B., Hungate, B. A., and Luo, Y.: Carbon-nitrogen interactions in terrestrial ecosystems
40 in response to rising atmospheric carbon dioxide, in: *Annual Review of Ecology Evolution and*
41 *Systematics*, *Annual Review of Ecology Evolution and Systematics*, 611-636, 2006.
- 42 Reich, P. B., and Hobbie, S. E.: Decade-long soil nitrogen constraint on the CO₂ fertilization of
43 plant biomass, *Nature Climate Change*, 3, 278-282, 10.1038/nclimate1694, 2013.

- 1 Rodell, M., Houser, P. R., Jambor, U., Gottschalck, J., Mitchell, K., Meng, C. J., Arsenault, K.,
2 Cosgrove, B., Radakovich, J., Bosilovich, M., Entin, J. K., Walker, J. P., Lohmann, D., and
3 Toll, D.: The global land data assimilation system, *Bulletin of the American Meteorological*
4 *Society*, 85, 381-394, doi:10.1175/bams-85-3-381, 2004.
- 5 Saikawa, E., Schlosser, C. A., and Prinn, R. G.: Global modeling of soil nitrous oxide emissions
6 from natural processes, *Glob. Biogeochem. Cycles*, 27, 972-989, doi:10.1002/gbc.20087, 2013.
- 7 Schlesinger, W. H.: On the fate of anthropogenic nitrogen, *Proceedings of the National*
8 *Academy of Sciences of the United States of America*, 106, 203-208,
9 doi:10.1073/pnas.0810193105, 2009.
- 10 Schmidt, J., Seiler, W., and Conrad, R.: Emission of nitrous oxide from temperate forest soils
11 into the atmosphere, *Journal of Atmospheric Chemistry*, 6, 95-115, 10.1007/bf00048334, 1988.
- 12 Schwalm, C. R., Williams, C. A., Schaefer, K., Baker, I., Collatz, G. J., and Roedenbeck, C.:
13 Does terrestrial drought explain global CO₂ flux anomalies induced by El Niño?,
14 *Biogeosciences*, 8, 2493-2506, doi:10.5194/bg-8-2493-2011, 2011.
- 15 Seneviratne, S. I., Corti, T., Davin, E. L., Hirschi, M., Jaeger, E. B., Lehner, I., Orlowsky, B.,
16 and Teuling, A. J.: Investigating soil moisture-climate interactions in a changing climate: A
17 review, *Earth-Sci. Rev.*, 99, 125-161, doi:10.1016/j.earscirev.2010.02.004, 2010.
- 18 Sheffield, J., Goteti, G., and Wood, E. F.: Development of a 50-year high-resolution global
19 dataset of meteorological forcings for land surface modeling, *J. Clim.*, 19, 3088-3111,
20 doi:10.1175/jcli3790.1, 2006.
- 21 Shevliakova, E., Pacala, S. W., Malyshev, S., Hurtt, G. C., Milly, P. C. D., Caspersen, J. P.,
22 Sentman, L. T., Fisk, J. P., Wirth, C., and Crevoisier, C.: Carbon cycling under 300 years of
23 land use change: Importance of the secondary vegetation sink, *Glob. Biogeochem. Cycles*, 23,
24 doi:10.1029/2007gb003176, 2009.
- 25 Sousa Neto, E., Carmo, J. B., Keller, M., Martins, S. C., Alves, L. F., Vieira, S. A., Piccolo, M.
26 C., Camargo, P., Couto, H. T. Z., Joly, C. A., and Martinelli, L. A.: Soil-atmosphere exchange
27 of nitrous oxide, methane and carbon dioxide in a gradient of elevation in the coastal Brazilian
28 Atlantic forest, *Biogeosciences*, 8, 733-742, doi:10.5194/bg-8-733-2011, 2011.
- 29 Stehfest, E., and Bouwman, L.: N₂O and NO emission from agricultural fields and soils under
30 natural vegetation: summarizing available measurement data and modeling of global annual
31 emissions, *Nutrient Cycling in Agroecosystems*, 74, 207-228, doi:10.1007/s10705-006-9000-
32 7, 2006.
- 33 Stocker, B. D., Roth, R., Joos, F., Spahni, R., Steinacher, M., Zaehle, S., Bouwman, L., Xu-Ri,
34 and Prentice, I. C.: Multiple greenhouse-gas feedbacks from the land biosphere under future
35 climate change scenarios, *Nature Climate Change*, 3, 666-672, doi:10.1038/nclimate1864, 2013.
- 36 Syakila, A., and Kroeze, C.: The global nitrous oxide budget revisited, *Greenhouse Gas*
37 *Measurement and Management*, 1, 17-26, doi:10.3763/ghgmm.2010.0007, 2011.
- 38 Thomas, R. Q., Brookshire, E. N. J., and Gerber, S.: Nitrogen limitation on land: how can it
39 occur in Earth system models?, *Global Change Biol.*, 21, 1777-1793, doi:10.1111/gcb.12813,
40 2015.
- 41 Thompson, R. L., Chevallier, F., Crotwell, A. M., Dutton, G., Langenfelds, R. L., Prinn, R. G.,
42 Weiss, R. F., Tohjima, Y., Nakazawa, T., Krummel, P. B., Steele, L. P., Fraser, P., O'Doherty,
43 S., Ishijima, K., and Aoki, S.: Nitrous oxide emissions 1999 to 2009 from a global atmospheric

1 inversion, *Atmospheric Chemistry and Physics*, 14, 1801-1817, doi:10.5194/acp-14-1801-2014,
2 2014.

3 Thornton, P. E., Lamarque, J.-F., Rosenbloom, N. A., and Mahowald, N. M.: Influence of
4 carbon-nitrogen cycle coupling on land model response to CO₂ fertilization and climate
5 variability, *Glob. Biogeochem. Cycles*, 21, doi:Gb4018 10.1029/2006gb002868, 2007.

6 van Groenigen, K. J., Osenberg, C. W., and Hungate, B. A.: Increased soil emissions of potent
7 greenhouse gases under increased atmospheric CO₂, *Nature*, 475, 214-U121,
8 doi:10.1038/nature10176, 2011.

9 Vitousek, P. M., Menge, D. N. L., Reed, S. C., and Cleveland, C. C.: Biological nitrogen
10 fixation: rates, patterns and ecological controls in terrestrial ecosystems, *Philosophical
11 Transactions of the Royal Society B-Biological Sciences*, 368, doi:10.1098/rstb.2013.0119,
12 2013.

13 Wei, Y., Liu, S., Huntzinger, D.N., Michalak, A.M., Viovy, N., Post, W.M., Schwalm, C.R.,
14 Schaefer, K., Jacobson, A.R., Lu, C., Tian, H., Ricciuto, D.M., Cook, R.B., Mao, J., and Shi,
15 X. : NACP MsTMIP: Global and North American Driver Data for Multi-Model
16 Intercomparison, Data set. Available on-line [<http://daac.ornl.gov>] from Oak Ridge National
17 Laboratory Distributed Active Archive Center, Oak Ridge, Tennessee, USA. Available at:
18 <http://dx.doi.org/10.3334/ORNLDAAC/1220> , 2014

19 Werner, C., Butterbach-Bahl, K., Haas, E., Hickler, T., and Kiese, R.: A global inventory of
20 N₂O emissions from tropical rainforest soils using a detailed biogeochemical model, *Glob.
21 Biogeochem. Cycles*, 21, GB3010, doi:10.1029/2006gb002909, 2007.

22 Xu-Ri, Wang, Y. S., Zheng, X. H., Ji, B. M., and Wang, M. X.: A comparison between
23 measured and modeled N₂O emissions from Inner Mongolian semi-arid grassland, *Plant and
24 Soil*, 255, 513-528, 2003.

25 Xu-Ri and Prentice, I. C.: Terrestrial nitrogen cycle simulation with a dynamic global
26 vegetation model, *Global Change Biology*, 14, 1745-1764, doi:10.1111/j.1365-
27 2486.2008.01625.x, 2008.

28 Xu-Ri, Prentice, I. C., Spahni, R., and Niu, H. S.: Modelling terrestrial nitrous oxide emissions
29 and implications for climate feedback, *New Phytologist*, 196, 472-488, doi:10.1111/j.1469-
30 8137.2012.04269.x, 2012.

31 Yienger, J. J., and Levy, H.: Empirical model of global soil-biogenic NO_x emissions, *J. Geophys.
32 Res.-Atmos.*, 100, 11447-11464, doi:10.1029/95jd00370, 1995.

33 Zaehle, S., and Friend, A. D.: Carbon and nitrogen cycle dynamics in the O-CN land surface
34 model: 1. Model description, site-scale evaluation, and sensitivity to parameter estimates, *Glob.
35 Biogeochem. Cycles*, 24, doi:10.1029/2009gb003521, 2010.

36 Zaehle, S., Friend, A. D., Friedlingstein, P., Dentener, F., Peylin, P., and Schulz, M.: Carbon
37 and nitrogen cycle dynamics in the O-CN land surface model: 2. Role of the nitrogen cycle in
38 the historical terrestrial carbon balance, *Global Biogeochemical Cycles*, 24,
39 doi:10.1029/2009gb003522, 2010.

40 Zaehle, S., Ciais, P., Friend, A. D., and Prieur, V.: Carbon benefits of anthropogenic reactive
41 nitrogen offset by nitrous oxide emissions, *Nat. Geosci.*, 4, 601-605, doi:10.1038/ngeo1207,
42 2011.

1 Zaehle, S., and Dalmonech, D.: Carbon-nitrogen interactions on land at global scales: current
2 understanding in modelling climate biosphere feedbacks, *Current Opinion in Environmental*
3 *Sustainability*, 3, 311-320, doi:10.1016/j.cosust.2011.08.008, 2011.

4 Zhuang, Q., Lu, Y., and Chen, M.: An inventory of global N₂O emissions from the soils of
5 natural terrestrial ecosystems, *Atmos. Environ.*, 47, 66-75,
6 doi:10.1016/j.atmosenv.2011.11.036, 2012.

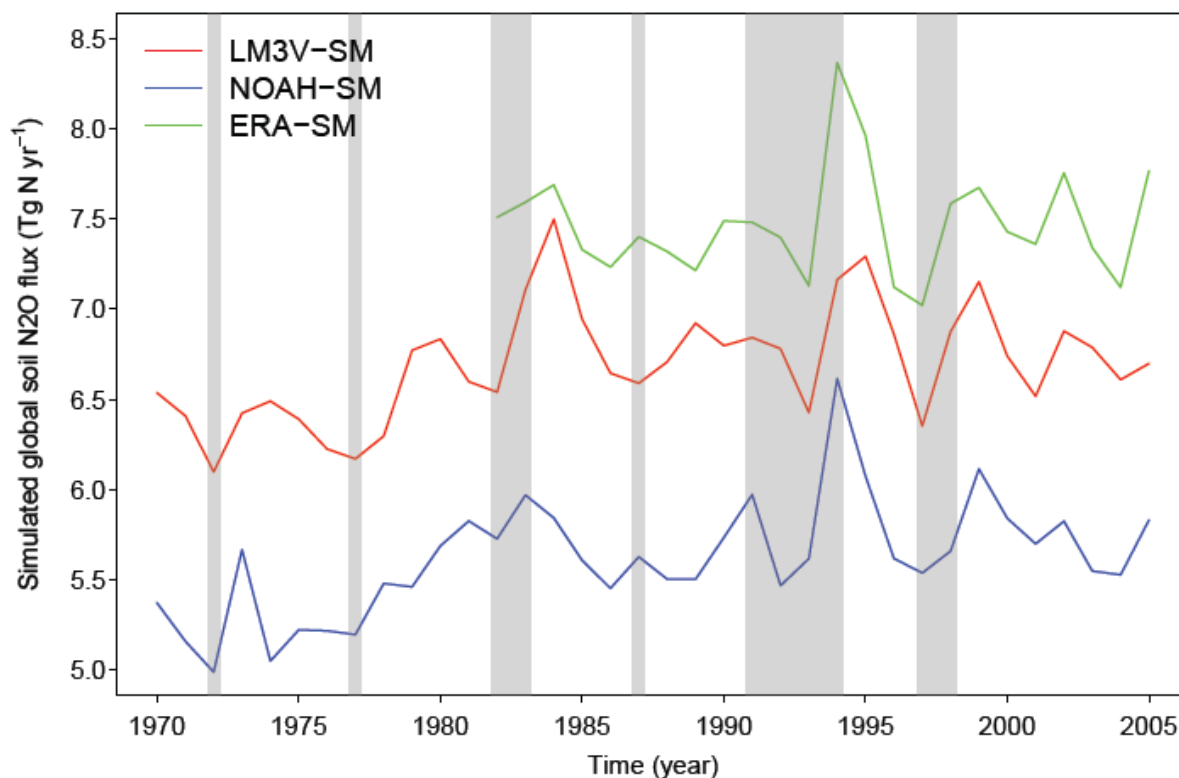
7

8

9

10

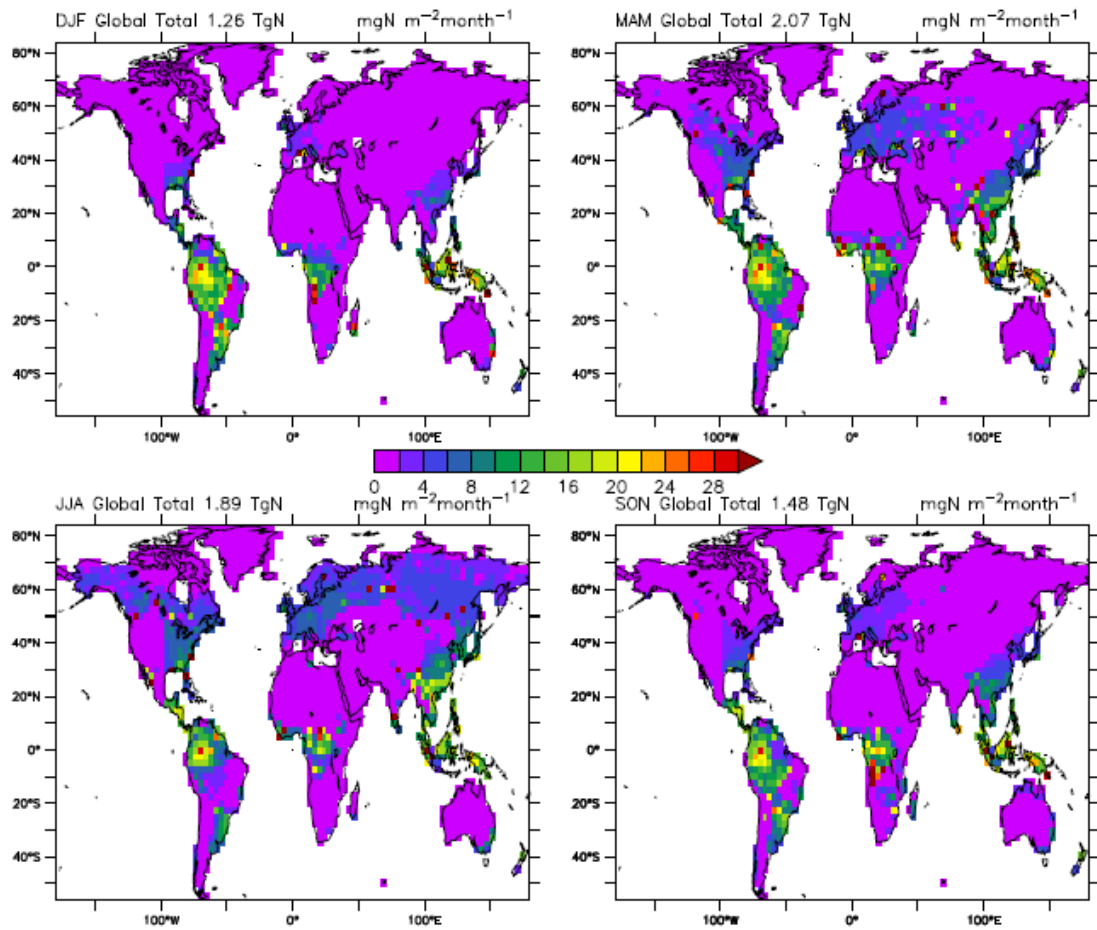
1 Figures and Tables



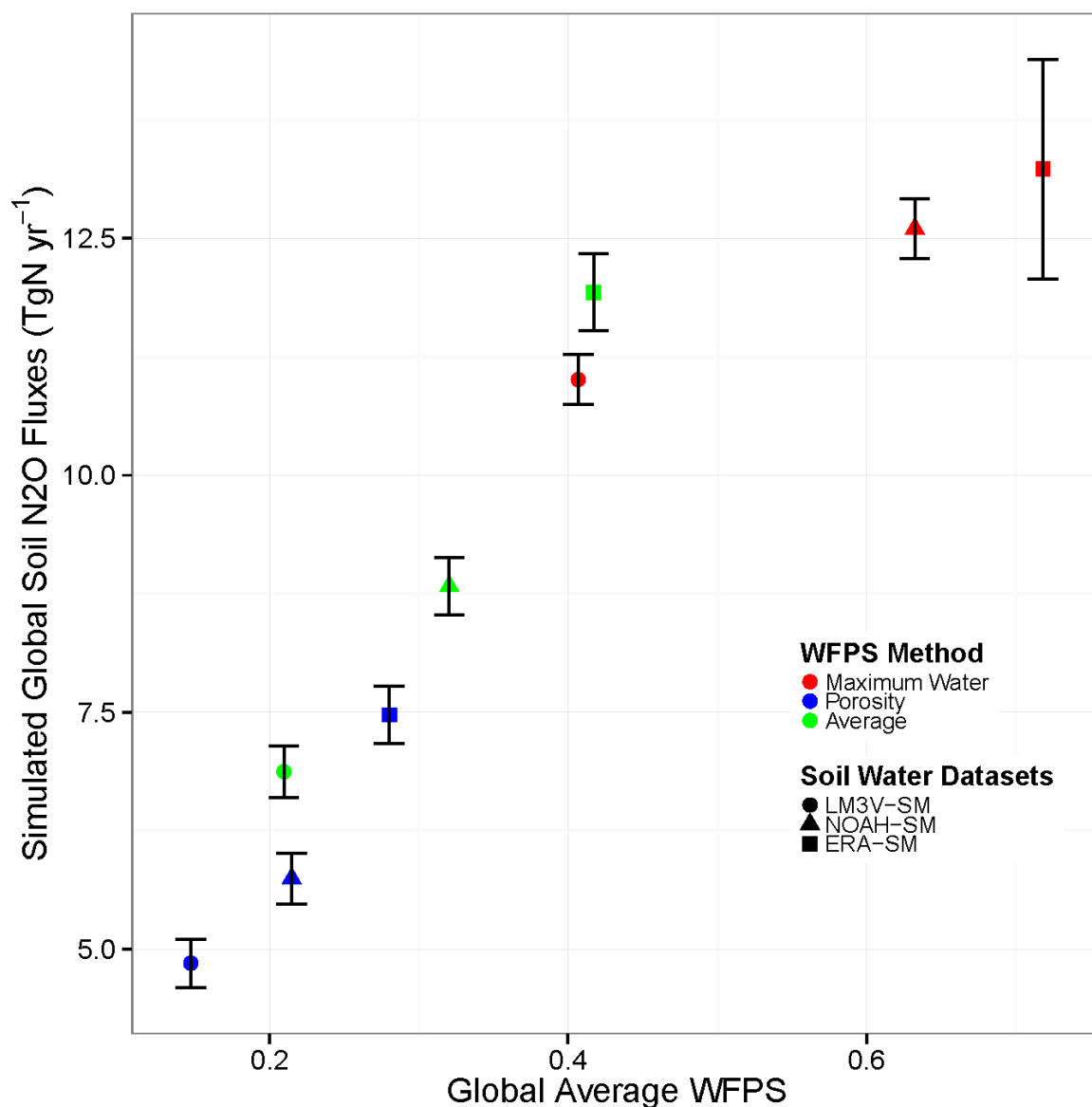
2

3 Figure 1. Simulated annual global soil N₂O emissions based on potential vegetation (1970-
4 2005). Shaded grey area indicates El Niño years with the annual multivariate ENSO index (MEI)
5 greater than 0.6. Colours refer to different soil moisture dataset used in the estimation: red for
6 LM3V-SM (with WFPS calculated by Method 3); blue for NOAH-SM (Method 2) and green
7 for ERA-SM (Method 2). Details for these soil moisture dataset and WFPS calculating methods
8 is available in the main text.

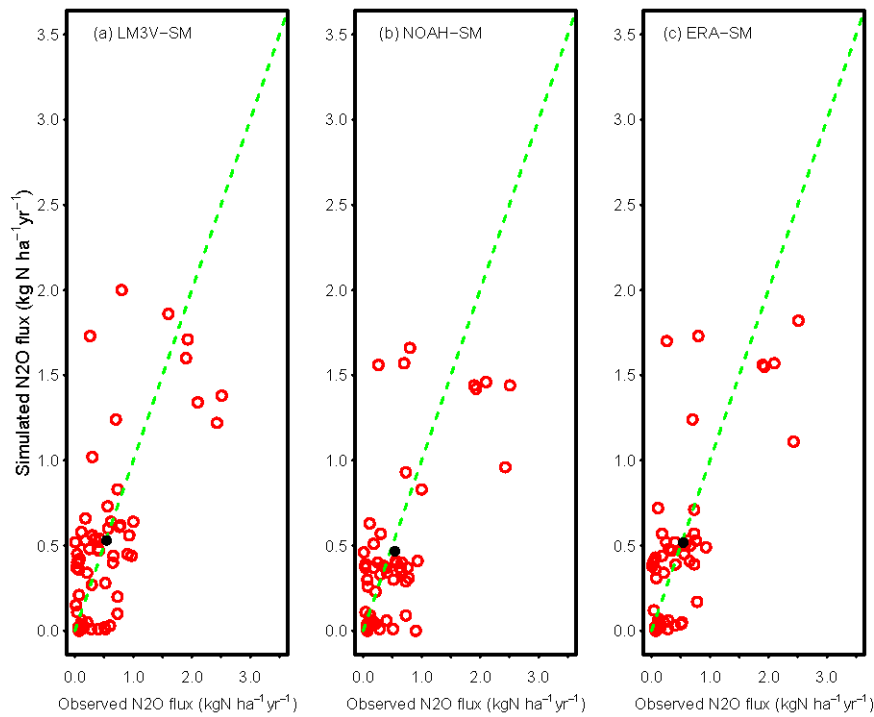
9



1
 2 Figure 2. Global seasonal mean soil N₂O emissions (with potential vegetation) averaged over
 3 the years 1970-2005. DJF (December, January and February), stands for Northern
 4 Hemisphere Winter; MAM (March, April and May) for Spring; JJA (June, July and August)
 5 for Summer; and SON (September, October and November) for Autumn.
 6



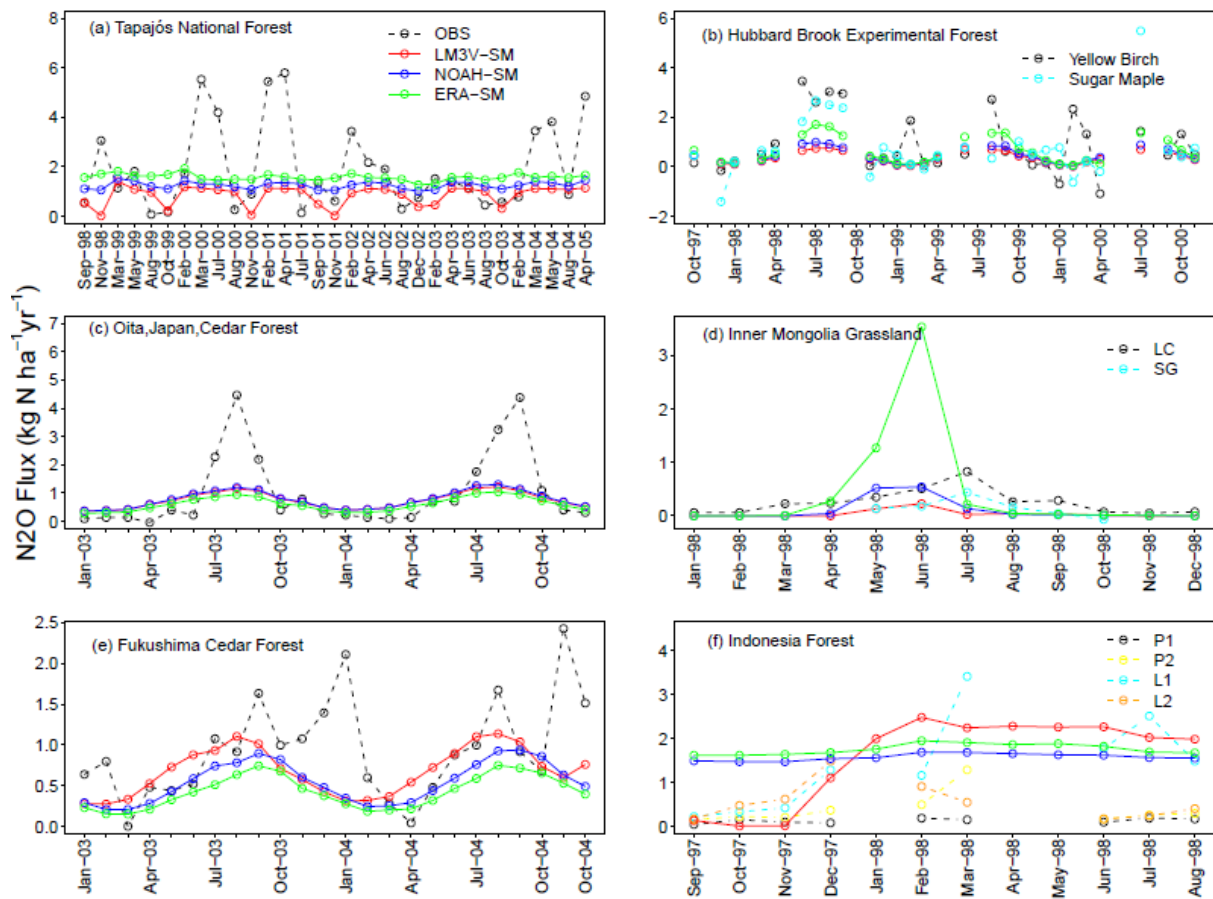
1
2 Figure 3. Sensitivity of simulated global soil N₂O emissions (with potential vegetation) to
3 water filled pore space (WFPS). The x-axis is the WFPS averaged globally over 1982-2005;
4 the y-axis represents the corresponding global total N₂O fluxes. A total of nine sets of WFPS
5 are obtained through either different soil water datasets (colours) or varied calculation
6 methods (symbols). Maximum water, porosity and average correspond to method 1, method 2
7 and method 3 in the main text, respectively. Coloured symbols represent interannual means
8 and error bars indicate interannual standard deviations.



1

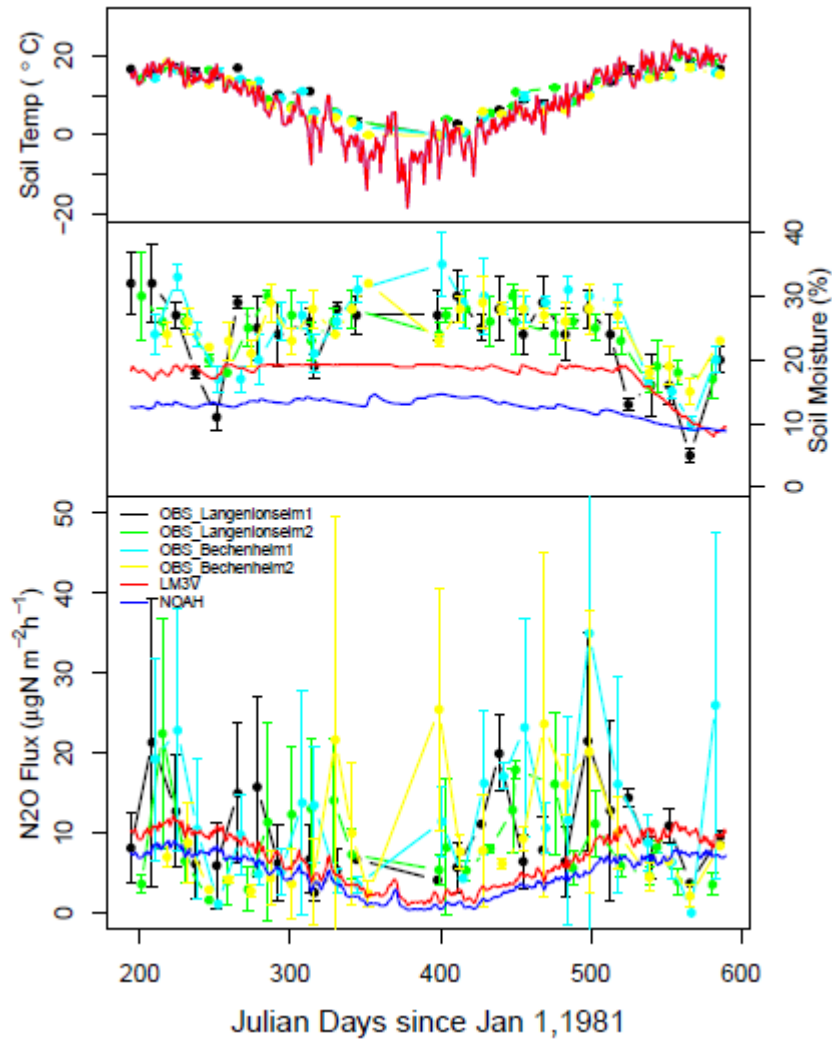
2 Figure 4. Observed vs. simulated annual N₂O emissions from natural soils. Dashed green lines
 3 are the 1:1 lines. The solid circles represent the overall means. Different panels represent
 4 simulations with different soil moisture data: (a) LM3V-SM (simulated by LM3V-N); (b)
 5 NOAH-SM (based on land surface model NOAH 3.3 in Global Land Data Assimilation System
 6 Version 2); and (c) ERA-SM (reanalysis data from ECMWF). Water filled pore space (WFPS)
 7 is calculated using the average of the one based on available water capacity and the one based
 8 on the total porosity (Method 3, see the main text for detailed description) for panel (a); and
 9 using the total porosity (Method 2) for panel (b) and (c).

10



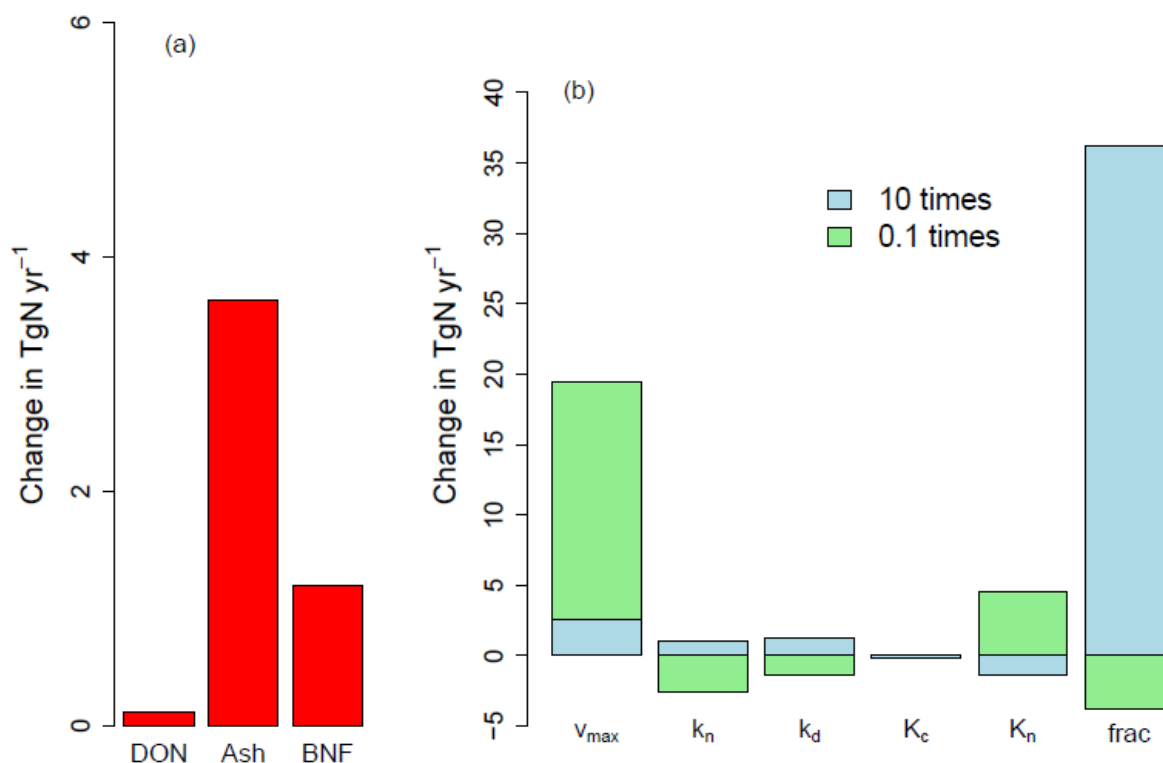
1
 2 Figure 5. Observed vs. simulated monthly N_2O emissions at (a), the Tapajós National Forest in
 3 east-central Amazonia ($3^{\circ}S$, $55^{\circ}W$), taken from Davidson et al. (2008); (b), the Hubbard Brook
 4 Experimental Forest in New Hampshire, USA ($44^{\circ}N$, $72^{\circ}W$), taken from Groffman et al. (2006);
 5 (c), a cedar forest at Oita, Japan ($33^{\circ}N$, $131^{\circ}E$), taken from Morishita et al. (2007) ; (d), the
 6 *Leymus chinensis* (LC) and *Stipa grandis* (SG) steppe in Inner Mongolia, China ($44^{\circ}N$, $117^{\circ}E$),
 7 taken from Xu-Ri et al. (2003); (e), a cedar forest in Fukushima, Japan ($37^{\circ}N$, $140^{\circ}E$), taken
 8 from Morishita et al. (2007); and (f), the primary (P1 and P2) and secondary (L1 and L2) forests
 9 located at the Pasir Mayang Research Site, Indonesia, taken from Ishizuka et al. (2002) ($1^{\circ}S$,
 10 $102^{\circ}E$). Shown are modeled results from three WFPS schemes (LM3V-SM, NOAH-SM and
 11 ERA-SM) the same as in Figure 4.

12
 13
 14



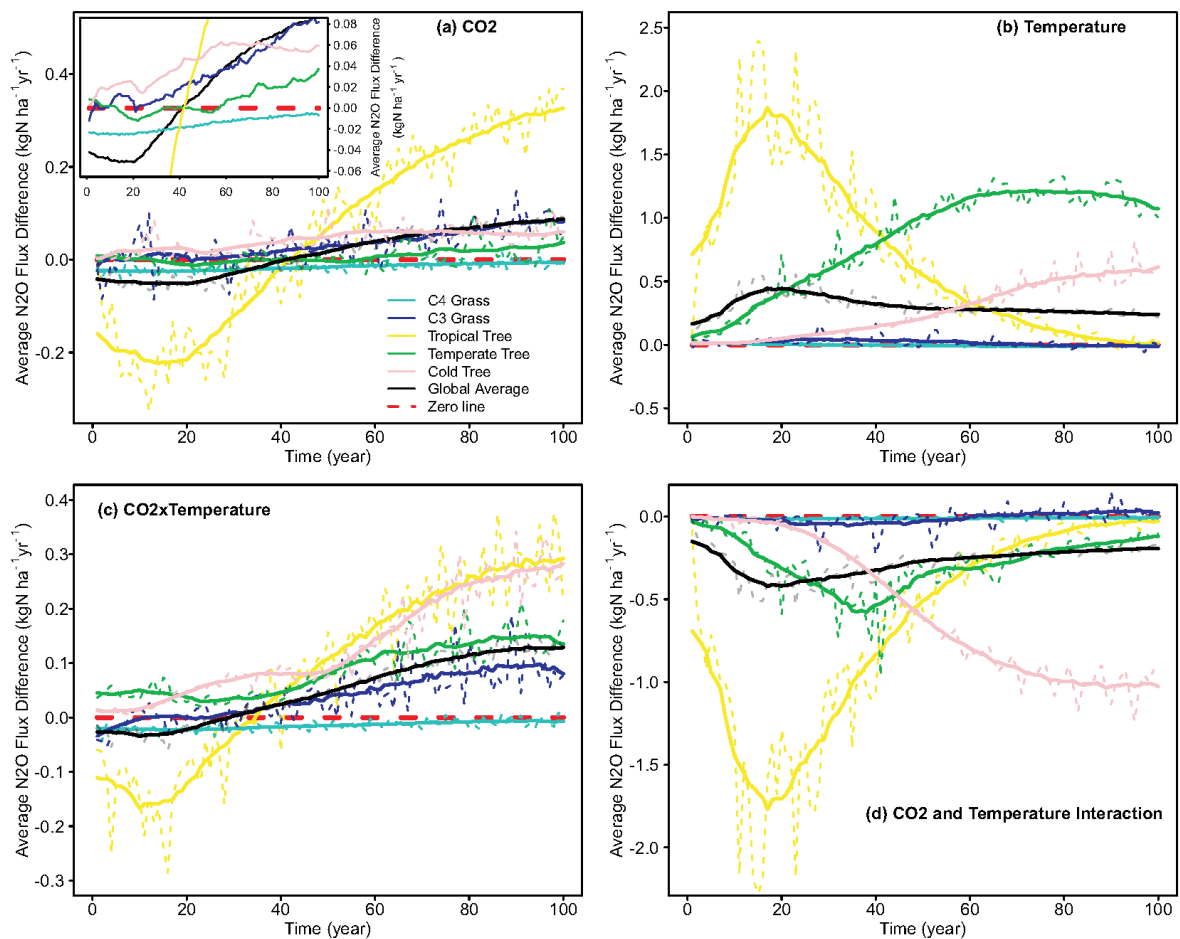
1
 2 Figure 6. Comparison of (a) soil temperature (2cm from observation and 1 cm from model)
 3 in °C; (b) soil moisture (2cm from observation and root zone from model) in % and (c) soil
 4 N₂O emissions in µgN m⁻² h⁻¹ from observations and model outputs at four forest sites from
 5 German (50°N, 8°E), taken from Schmidt et al. (1986). Shown are modeled results from two
 6 WFPS schemes (LM3V-SM and NOAAH-SM) similar as in Figure 4.

7
 8

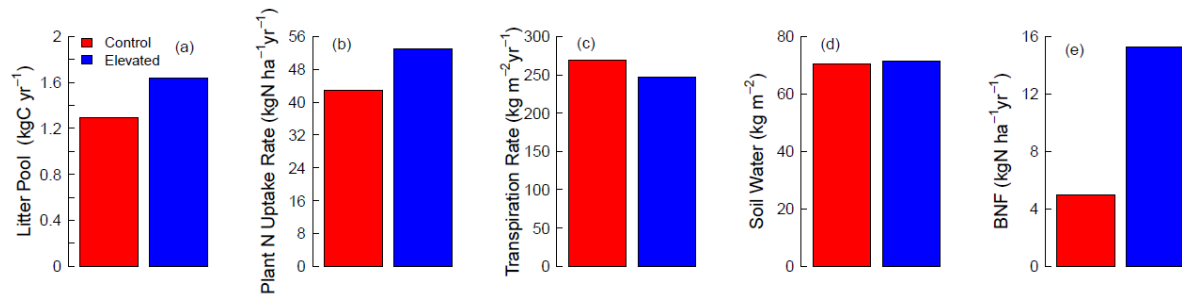


1
 2 Figure 7. Changes in simulated global average N₂O (1950-2005) emissions from modifying
 3 general N cycling processes (a) and model parameters one-at-a-time (b). Altered processes
 4 include disallowing N losses through dissolved organic matter (DON in (a)) and fire
 5 volatilization (Ash in (a)), and replacing simulated biological N fixation with preindustrial N
 6 fixation rate (BNF in (a)). Parameters include: v_{max} , the maximum active N uptake rate per unit
 7 root biomass; k_n , the optimum nitrification rate; k_d , the optimum denitrification rate; K_c and K_n ,
 8 the half saturation constants for labile C availability and nitrate respectively; and $frac$ is the
 9 fraction of net nitrification lost as N₂O. Parameters are either increased by multiplying 10
 10 (lightblue) or reduced by multiplying 0.1 (lightgreen) relative to the defaults .

11
 12
 13



1
 2 Figure 8. Soil N₂O emissions in response to step increases in atmospheric CO₂ and temperature.
 3 Panel (a) is the response to CO₂ fertilization alone, expressed as the difference between CO₂
 4 increased run and the control run (CO₂_FERT - CONTROL), the inset zooms into the y axis
 5 (flux difference) around zero; Panel (b) is the response to temperature increase alone (TEMP-
 6 CONTROL); Panel (c) is the combined response to both CO₂ enrichment and temperature rise
 7 (CO₂_FERT×TEMP-CONTROL); and Panel (d) is the interactive effect of CO₂ and
 8 temperature responses, which is the difference between the combined (results from Panel (c))
 9 and minus the individual responses (results from Panel (a) and (b)). Results are shown as annual
 10 values (thin dashed lines) and as running average with a moving window of 17 years (period of
 11 recycled climate forcing, thick solid lines) . The black lines represent the global average
 12 response. Coloured lines indicate responses for biome as represented by each plant functional
 13 type (PFT) considered in LM3V-N: C4 grass (cyan), C3 grass (blue), tropical forest (yellow),
 14 temperate deciduous forest (green) and cold evergreen forest (pink). Dashed red line represents
 15 the zero line.



1
 2 Figure 9. CO₂ fertilization effects (no temperature change) on litter pool size (Panel (a)), plant
 3 nitrogen uptake rate (Panel (b)), canopy transpiration rate (Panel (c)), soil water content in the
 4 root zone (Panel (d)) and biological nitrogen fixation (BNF) rate (Panel (e)). Shown are the
 5 100-year average of global means (spatial) for control (284 ppm, red) and with elevated CO₂
 6 (568 ppm, blue).

7

8 Table 1 Texture dependent parameter *k* estimated from Del Grosso et al. (2000)

Soil Texture	Coarse	Medium	Fine	Coarse/medium	Coarse/fine	Medium/fine	Coarse/medium/fine	Organic
<i>k</i>	2	10	22	6	12	16	11	2

9

10